

# Breakdown of the Hard Thermal Loop expansion near the light-cone

P. Aurenche<sup>1,2,a,b</sup>, F. Gelis<sup>2,c</sup>, R. Kobes<sup>3,d</sup>, E. Petitgirard<sup>3,e</sup>

August 5, 2018

1. CFIF, Instituto Superior Técnico, Edifício Ciência (física), P-1096 Lisboa, Codex, Portugal
2. Laboratoire de Physique Théorique ENSLAPP, B.P. 110, F-74941 Annecy-le-Vieux Cedex, France
3. Physics Department and Winnipeg Institute for Theoretical Physics, University of Winnipeg, Winnipeg, Manitoba R3B 2E9, Canada

## Abstract

We discuss the bremsstrahlung production of soft real and virtual photons in a quark-gluon plasma at thermal equilibrium beyond the Hard Thermal Loop (HTL) resummation. The physics is controlled by the ratio  $Q^2/q_0^2$  of the virtuality to the energy. When  $Q^2/q_0^2 \ll g^2$ , where  $g$  is the strong coupling constant, the emission rate is enhanced by a factor  $1/g^2$  over the HTL results due to light-cone singularities and the bremsstrahlung is induced by scattering of the quark via both transverse and longitudinal soft gluon exchanges. When  $Q^2/q_0^2$  increases, the enhancement factor is given by  $q_0^2/Q^2$ . When this ratio is near unity, the bremsstrahlung contribution is of the same order as the rate predicted by the HTL resummation. In that case, the bremsstrahlung is induced by both soft and hard gluon exchanges.

ENSLAPP-A-614/96, WIN-96-13, hep-ph/9609256

---

<sup>a</sup>On leave of absence from ENSLAPP, B.P. 110, F-74941 Annecy-le-Vieux Cedex, France

<sup>b</sup>aurenche@lapp.in2p3.fr, <sup>c</sup>gelis@lapp.in2p3.fr

<sup>d</sup>randy@theory.uwinnipeg.ca, <sup>e</sup>petitg@theory.uwinnipeg.ca

# 1 Introduction

Several methods have recently been used for calculating the rate of soft real or virtual photons in a hot quark-gluon plasma. These methods lead to drastically different physical pictures and orders of magnitude for the calculated rates. In the following we will always assume the plasma to be in thermal equilibrium and the QCD coupling constant  $g \ll 1$ . We furthermore assume that the produced photon does not interact with the quark-gluon plasma due to the smallness of the electric charge  $e$  compared to the strong interaction coupling: in other words the photon is not thermalized.

In the hard thermal loop (HTL) resummation analysis [1, 2, 3] the photon is radiated off in processes which always involve an interaction between the plasma particles which are dominated by soft (energy  $\sim gT$ ) quasi-fermion exchanges [4]. In the case of real photon emission, a strict application of the HTL rules leads to a prediction with a logarithmic singularity associated to collinear divergences [5, 6].

In a semi-classical approach [7, 8, 9], the photon is radiated off by a hard quark (energy  $\sim T$ ) interacting with quarks and gluons in the plasma via the exchange of soft gluons, the interactions being assumed to be screened by the Debye mass. Multiple re-interactions of the radiating quark in the plasma regularize potential collinear singularities in the lowest order process and, more importantly, suppress the photon spectrum at small frequencies due to the Landau-Pomeranchuk-Migdal (LPM) effect [10]. For a different approach of this effect, see [11, 12].

The regularization of divergences in the bremsstrahlung process has also been achieved, under somewhat different hypotheses, by the resummation of soft photon emission with a single interaction of the radiating quark in the plasma [13, 14]. We will not consider this possibility as it affects the photon spectrum at very small momenta, of order  $eT$ , while we are interested here in momenta of order  $gT$ .

In the following, we come back to the problem of real or virtual soft photon emission, in the framework of thermal field theory, showing the necessity of going beyond the HTL approximation for obtaining consistent predictions. The picture which emerges is rather different from the above quoted results. Compared to the HTL approach we find, in fact, that there is no contribution from hard thermal loops at the expected leading order in  $g$ . However some non leading terms in the HTL approximation become enhanced by singularities near the light-cone and dominate over the would-be HTL order [15]. In the case of real or quasi-real photons (virtualities  $Q^2/q_0^2 \ll 1$ ) the dominant diagrams are the bremsstrahlung ones in agreement with the hypotheses of [7, 8, 9] and we find that, for  $Q^2/q_0^2 \leq g^2$ , the production rate is  $R \sim e^2 g^4 T^4 / q_0^2$  modulo some logarithmic factor. The results are shown to be independent of the covariant gauge parameter. Unlike in [7, 8, 9] we treat the interaction between quarks and gluons in the plasma “exactly”, in the framework of thermal field theory, and we do not find that the static approximation is a good one as exchanges of “magnetic” gluons are as important as that of “electric” ones.

In summary, the result of our analysis concerns photons of momentum much less than  $T$  radiated by hard quarks in a plasma: for virtualities  $Q^2/q_0^2 \ll 1$  we find an enhancement, due to light-cone singularities, over the rate  $R \sim e^2 g^4 T^4 / q_0^2$  (modulo logarithmic factors) expected in the HTL approximation; for virtualities  $Q^2/q_0^2 \sim 1$  no enhancement occurs but the bremsstrahlung contributions are of the same order as the “soft-fermion” contributions calculated in [4]. This extends out of the light-cone our previous results on photon production on the light-cone [15].

Problems in the HTL expansion associated to light-cone singularities have already been discussed several times in the literature: as mentioned above they render the rate of soft real photon production

logarithmically divergent [5, 6, 16]. In fact, already in their original paper [2] Braaten and Pisarski discuss mass divergences, *i.e.* terms such as  $g^2 T/(\omega - p)$  with  $\omega \rightarrow p$ , and they mention that these terms could spoil the HTL expansion. In order to solve this problem it has been proposed recently [17, 18, 19] to extend the HTL action to include thermal corrections (essentially the effective thermal mass) on hard propagators but no general proof exists that this improvement is sufficient or complete. A particularly interesting feature of the problem we consider here is that the mass singularities change the expected order of the leading HTL prediction and enhance it by a factor which may be as large as  $1/g^2$  in some cases.

## 2 Discussion of the existing approaches

This part is devoted to a critical appraisal of the previous calculations of the real and virtual photon production rates in a quark-gluon plasma.

### 2.1 Weaknesses of the Hard Thermal Loop expansion

One of the first applications of the HTL resummation scheme was the calculation of the production rate of a soft photon, of virtuality  $Q^2$ , at rest in a quark-gluon plasma [4]. Before resummation is taken into account, the photon is produced by the annihilation of a soft quark-antiquark pair in the plasma. The imaginary part of the vacuum polarization diagram, which is proportional to the invariant production rate  $R$  up to a statistical weight, is found to be

$$\text{Im}\Pi^\mu{}_\mu(Q) \sim e^2 Q^2 (1 - 2n_F(\frac{Q}{2})) \sim e^2 g^3 T^2 \quad \text{for } q, q_0 \sim gT \quad (1)$$

In the HTL approach the diagrams to be calculated are shown in Fig. 1. In fact, only the first one, with effective quark propagators and effective  $q - \bar{q} - \gamma^*$  vertices, is said to contribute: the self-energy diagram with the gluon loop in fact does not exist because there is no  $g - g - \gamma$  effective vertex (Furry's theorem) and the two tadpole diagrams vanish because the traces of the corresponding 4-point effective vertices also vanish. A compact expression, involving convolutions of the effective soft fermion spectral functions has been obtained by Braaten, Pisarski and Yuan [4] and one can estimate the order of magnitude of their result to be as in Eq. (1). An important fact concerns the statistical factor  $(1 - 2n_F(\frac{Q}{2}))$  associated to the annihilating  $q$  and  $\bar{q}$  which becomes  $(1 - n_F(\omega) - n_F(\frac{Q}{2} - \omega))$ , where  $\omega$  is the energy of one of the annihilating soft fermion in the HTL approach: for soft energies it brings an extra suppression factor  $g$  to the photon production rate.

Consider now, for example, the last diagram with the gluon tadpole and in particular the order of  $\Pi^{00}$  or  $\Pi^{ij}$ . Using the HTL rules, the  $g - g - \gamma - \gamma$  effective vertex is found to be of order  $e^2$  while the soft effective gluon loop yields [2]

$$\int_{\text{soft } k} d^3 k \frac{n_B(k)}{k} \sim gT^2 \quad (2)$$

because of the enhancement due to the Bose-Einstein statistical factor  $n_B(k)$ . We then find

$$\Pi^{00} \sim \Pi^{ij} \sim e^2 gT^2. \quad (3)$$

Of course, we have a cancelation when taking the trace  $\Pi^\mu{}_\mu$ : this is why this diagram is said to be vanishing in the HTL framework. The important point is that the vanishing of the HTL contribution occurs in this diagram at the order  $e^2 g T^2$  while the calculated soft fermion loop contribution is of order  $e^2 g^3 T^2$ . Therefore, non-leading terms (in the HTL sense) in the gluon tadpole may be as large as the soft fermion loop contribution. This is indeed the case and these non-leading terms will play a very important role. A similar discussion may be given concerning the fermion tadpole Fig. 1-(c) which should however be suppressed by a power of  $g$  compared to Fig. 1-(d) because of the lack of Bose-Einstein enhancement at soft momenta.

In terms of physical processes Fig. 1-(a) involves the first three amplitudes shown in Fig. 2 (and their crossing symmetric ones) where the photon is radiated off either by a soft quasi-fermion (a) or by a hard on shell fermion (b and c): the imaginary part of Fig. 1-(a) is in fact constructed from squaring Fig. 2-(a) or taking the interference of (a),(b) and (c). On the other hand “squaring” the diagram Fig. 2-(b) or (c) yields the soft fermion tadpole diagram of Fig. 1-(c). In all cases though, the interactions between hard particles in the plasma are mediated by soft fermion exchanges. The absence of processes where a gluon is exchanged between the partons in the plasma, which are intuitively expected to be relevant, seems to indicate that the calculation based on the soft fermion loop is not complete. The expected amplitudes are, in fact, contained in Fig. 1-(d) and are obtained when “cutting” through the effective gluon and the effective 4-point function: these are shown in Fig. 2-(d) and (e). In this set of diagrams the hard gluon line can be replaced by a hard quark line, since the radiating quark can be scattered by any kind of parton in the plasma. The physical process involved is the bremsstrahlung of the photon by a hard quark which scatters in the plasma via the exchange of a soft gluon. The calculation of the diagram of Fig. 1-(d), in thermal field theory, will be the main purpose of this paper and it will be found that indeed its contribution to  $\text{Im } \Pi^\mu{}_\mu$  is at least of order  $e^2 g^4 T^3 / q_0$  and that, in the case of quasi-real photons, of virtuality  $Q^2 / q_0^2 \ll 1$ , it is further enhanced by powers of  $1/g$ .

To be complete, one should also mention that the soft fermion loop contribution to real photon production has been calculated [5, 6] and the result is as in Eq. (1) with the added feature of logarithmic mass singularities due to the emission of the photon collinear to the hard massless quark. These singularities are regularized by giving the quark its asymptotic thermal mass [16].

## 2.2 Semi-classical approach: LPM effect

The diagrams of Fig. 2-(d) and (e) have been considered in a series of papers by Cleymans, Goloviznin and Redlich [7, 8, 9]. In fact, the purpose of these works was to study the effect of multiple rescattering of the radiating quark in the plasma: they find that even when working with massless quarks the rate of production of on-shell photons is finite due to rescattering effects, and, more importantly, they show that the shape of the photon spectrum is modified, at small energies, and becomes  $1/\sqrt{q_0}$  rather than the usual logarithmically divergent bremsstrahlung spectrum in  $1/q_0$ : this is an illustration of the Landau-Pomeranchuk-Migdal effect [10]. The results of [7, 8, 9] are obtained in the semi-classical approximation (the quark follows a classical path) and it is assumed that the interaction of the quark in the plasma is as at  $T = 0$ , the only thermal input being the Debye mass, introduced by hand to regularize the forward singularity of the quark scattering amplitude. With the LPM effect taken into account their result yields  $\text{Im } \Pi^\mu{}_\mu \sim e^2 g^2 T^2 (T/q_0)^{1/2}$ , whereas without the LPM effect, the case we concentrate upon below, one obtains  $\text{Im } \Pi^\mu{}_\mu \sim e^2 g^2 T^3 / q_0$ . We will come back to a detailed comparison

of this result with our calculation after our results have been presented.

### 3 Generalities of the calculation

This section is devoted to explain the notations and to give general results to be used later whatever the virtuality of the emitted photon is.

#### 3.1 Some notations and preliminaries

The invariant rate of production, per unit time and per unit volume of the plasma, of a real photon is given to first order in  $\alpha$  (*i.e.* this formula takes only into account the emission by a quark of a single photon, but does not consider the possibility of emitting more than one photon) by [20]:

$$R \equiv q_0 \frac{dN}{d^3q d^4x} = -\frac{1}{(2\pi)^3} n_B(q_0) \text{Im} \Pi^\mu{}_\mu(Q). \quad (4)$$

For a lepton pair of invariant mass squared  $Q^2$  the rate, integrated over the leptons kinematical variables, is

$$\frac{dN}{dq_0 d^3q d^4x} = -\frac{\alpha}{12\pi^3} \frac{1}{Q^2} n_B(q_0) \text{Im} \Pi^\mu{}_\mu(Q). \quad (5)$$

It is worth noticing that these formulae, although giving only the dominant term in  $\alpha$  of the quark, are exact to all orders in  $\alpha_s$ . We will need to compute the imaginary part of the photon self-energy, which is given at lowest order in  $\alpha_s$  by the two loop diagrams of Fig. 3, to which one should also add the diagram with the self-energy correction on the upper fermion line (not represented). These diagrams are an explicit representation of the gluon tadpole of Fig. 1-(d) and, as explained before, they will be calculated beyond the HTL approximation. In the following, a summation over the transverse (T), longitudinal (L) and gauge dependent (G) modes in the gluon propagator is always assumed.

The notations for the momenta are explained in Fig. 3. In the kinematical domain we consider, the fermion in the loop has a hard momentum, which means that the components of its momentum are of order  $T$ , and the exchanged gluon as well as the external photon have momentum components much smaller than  $T$ .

##### 3.1.1 The “retarded-advanced” formalism

In order to compute the needed imaginary part, we will proceed by using the “retarded-advanced” formalism [21, 22, 23], which is one of the simplest versions of the real-time formalisms. This formalism is obtained from the more common “1-2” formalism [24, 25, 26, 27] by a change of basis. The result of such a transformation is a formalism with a new  $2 \times 2$  matrix propagator and new vertices. A nice feature of the “retarded-advanced” formalism lies in the fact that it takes into account, in an optimal way, the Kubo-Martin-Schwinger identities valid at thermal equilibrium, so that among the four components of the matrix propagator only two are non zero; more precisely, the matrix propagator

we get for a real scalar field is (for fermions or gauge fields, one has to take into account also the Dirac or Lorentz structure):

$$\Delta(P) = \begin{pmatrix} \Delta_R(P) & 0 \\ 0 & \Delta_A(P) \end{pmatrix}, \quad (6)$$

where the retarded and advanced propagators are given by

$$\Delta_{R,A}(P) \equiv \frac{i}{P^2 - M^2 \pm i\epsilon p_0}, \quad \epsilon > 0. \quad (7)$$

Another feature of this matrix propagator is that it no longer contains any information relative to the thermal equilibrium. Of course, as said before, the change of basis for the propagator has as a consequence a change in the vertices to be used, and the price to pay for these simple propagators is somewhat intricate vertices. For example, for a *QED*-like vertex with entering momenta  $P, Q$  and  $-R, Q$  being the photon momentum, we have:

$$\begin{aligned} g_{AAA}(P, Q, -R) &= g_{RRR}(P, Q, -R) = 0, \\ g_{RRA}(P, Q, -R) &= g_{ARR}(P, Q, -R) = g_{RAR}(P, Q, -R) = e, \\ g_{RAA}(P, Q, -R) &= -e (1 + n_B(q_0) - n_F(r_0)), \\ g_{ARA}(P, Q, -R) &= -e (1 - n_F(p_0) - n_F(r_0)), \end{aligned} \quad (8)$$

where  $n_B(q_0) \equiv 1/(e^{\beta q_0} - 1)$ ,  $n_F(p_0) \equiv 1/(e^{\beta p_0} + 1)$ , and  $\beta \equiv 1/T$  is the inverse temperature. Therefore, in this formalism, all the thermal information is put into the vertices. The thermal content of an  $n$ -point function is represented by the external  $R/A$  indices. Inside a loop a sum is made over the internal thermal indices with appropriate internal propagators joining them.

### 3.1.2 Effective soft gluon propagator

Since the exchanged gluons can be soft in our diagrams, we will need to use effective propagators taking into account the Hard Thermal Loop corrections [2, 3]. We choose to use a covariant gauge in which the effective gluon propagator is decomposed into its transverse, longitudinal and gauge components:

$$-D^{\mu\nu}(L) \equiv P_T^{\mu\nu}(L)\Delta^T(L) + P_L^{\mu\nu}(L)\Delta^L(L) + \xi P_G^{\mu\nu}(L)\Delta^G(L), \quad (9)$$

where  $\xi$  is the gauge parameter, and with

$$\begin{aligned} \Delta^{T,L}(L) &\equiv \frac{i}{L^2 - \Pi_{T,L}(L)} \\ \Delta^G(L) &\equiv \frac{i}{L^2}. \end{aligned} \quad (10)$$

The appropriate choice of  $l_0 \pm i\epsilon$  is implicitly understood when considering R, A propagators. The tensors  $P_{T,L,G}^{\mu\nu}(L)$  are the transverse, longitudinal and gauge projectors whose explicit expression are [27, 28, 29, 30]

$$\begin{aligned} P_T^{\mu\nu}(L) &= \gamma^{\mu\nu} - \frac{\kappa^\mu \kappa^\nu}{\kappa^2} \\ P_L^{\mu\nu}(L) &= U^\mu U^\nu + \frac{\kappa^\mu \kappa^\nu}{\kappa^2} - \frac{L^\mu L^\nu}{L^2} \\ P_G^{\mu\nu}(L) &= \frac{L^\mu L^\nu}{L^2} \end{aligned} \quad (11)$$

where  $\gamma^{\mu\nu} \equiv g^{\mu\nu} - U^\mu U^\nu$ ,  $\kappa^\mu \equiv \gamma^{\mu\nu} L_\nu$ , and where  $U$  is the mean velocity of the plasma in the current frame. As is usual, in the following we will work in the rest-frame of the plasma in order to have simpler expressions.

The explicit form of the functions  $\Pi_{T,L}(L)$  are [28, 29]

$$\begin{aligned}\Pi_T(l, l_0) &= 3m_g^2 \left[ \frac{x^2}{2} + \frac{x(1-x^2)}{4} \ln \left( \frac{x+1}{x-1} \right) \right] \\ \Pi_L(l, l_0) &= 3m_g^2 \left[ (1-x^2) - \frac{x(1-x^2)}{2} \ln \left( \frac{x+1}{x-1} \right) \right]\end{aligned}\quad (12)$$

where  $x \equiv l_0/l$  and  $m_g^2 \equiv g^2 T^2 [N + N_f/2]/9$  is the gluon thermal mass in a  $SU(N)$  gauge theory with  $N_f$  flavors. Since these functions depend only of  $x = l_0/l$ , we will often simplify the notation by simply indicating  $x$  in their list of arguments.

It will be useful to introduce the spectral functions

$$\rho_{T,L}(l, l_0) \equiv \frac{i}{L^2 - \Pi_{T,L}(L)} \Big|_R - \frac{i}{L^2 - \Pi_{T,L}(L)} \Big|_A. \quad (13)$$

The properties of these spectral functions are closely related to the analytic structure of the gluon propagator. In particular, this propagator possesses two thermal mass-shells (a transverse one and a longitudinal one) above the light-cone, determined by the equation  $L^2 = \Pi_{T,L}(L)$ , and to which correspond delta functions in  $\rho_{T,L}$  for  $L^2 > 0$ . When  $L^2 < 0$  (*i.e.*  $|x| < 1$ ), the self-energies  $\Pi_{T,L}(L)$  acquire an imaginary part due to the logarithm (a phenomenon known as Landau damping), so that the corresponding contribution in  $\rho_{T,L}$  is:

$$\frac{-2\text{Im} \Pi_{T,L}(L)|_R}{\left(L^2 - \text{Re} \Pi_{T,L}(L)\right)^2 + \left(\text{Im} \Pi_{T,L}(L)|_R\right)^2}. \quad (14)$$

For completeness we give here the value of the imaginary parts to be used later:

$$\begin{aligned}\text{Im} \Pi_T(L)|_R &= \frac{3\pi m_g^2}{4} x(1-x^2) \\ \text{Im} \Pi_L(L)|_R &= -2 \text{Im} \Pi_T(L)|_R.\end{aligned}\quad (15)$$

### 3.1.3 Resummed hard fermion propagator

Since the calculation done with massless fermions leads to collinear divergences [15], it has been proposed in [17] to cure these singularities by taking into account the thermal mass even for hard particles. Without any approximation, this resummed propagator reads [29, 30, 31]:

$$\mathcal{S}(P) = \frac{i}{2} \left[ \frac{\gamma^0 - \hat{p} \cdot \vec{\gamma}}{(p_0 - \Sigma_0(P)) - \|\vec{p} - \vec{\Sigma}(P)\| + i\epsilon} + \frac{\gamma^0 + \hat{p} \cdot \vec{\gamma}}{(p_0 - \Sigma_0(P)) + \|\vec{p} - \vec{\Sigma}(P)\| - i\epsilon} \right], \quad (16)$$

where, at the one loop order,

$$\begin{aligned}\Sigma_0(P) &= \frac{M_\infty^2}{4p} \ln\left(\frac{x+1}{x-1}\right) \\ \vec{\Sigma}(P) &= \hat{p} \frac{M_\infty^2}{2p} \left[1 - \frac{x}{2} \ln\left(\frac{x+1}{x-1}\right)\right]\end{aligned}\quad (17)$$

with  $x \equiv p_0/p$ , and where  $M_\infty^2 \equiv g^2 C_F T^2/4$  stands for the asymptotic fermion thermal mass.

It is well known that this resummed propagator possesses two mass-shells (usually denoted by + and -), the energy of which can be approximated for hard  $p$  by:

$$\begin{aligned}\omega_+(p) &\underset{p \sim T}{\approx} \sqrt{p^2 + M_\infty^2} \\ \omega_-(p) &\underset{p \sim T}{\approx} p \left(1 + 2 \exp\left(-4p^2/M_\infty^2 - 1\right)\right)\end{aligned}\quad (18)$$

Moreover, the residue associated to the - pole is exponentially small whereas the residue associated to the + pole is approximately 1. This means that in a momentum integral involving such a propagator and where  $p$  is hard, we need only to take into account the + pole. In such circumstances, the resummed fermion propagator can be simplified to get:

$$\mathcal{S}(P) \approx i \frac{p_0 \gamma^0 - \omega_+(p) \hat{p} \cdot \vec{\gamma}}{p_0^2 - \omega_+^2(p) + i\epsilon} \approx \not{P} S(P), \quad (19)$$

where

$$S(P) \equiv \frac{i}{P^2 - M_\infty^2 + i\epsilon}. \quad (20)$$

### 3.2 Expression of $\text{Im}\Pi^\mu{}_\mu$

Armed with these tools, one can now evaluate the imaginary part of the diagrams represented on Fig. 3. The imaginary part of the photon self-energy is related to the retarded and advanced ones by

$$2i \text{Im}\Pi^\mu{}_\mu = \Pi^\mu{}_{\mu|R} - \Pi^\mu{}_{\mu|A} \quad (21)$$

In order to simplify the expressions, we will forget for a while all the color and group factors, and reintroduce them only at the end of the calculation.

Let us begin by the self-energy correction of Fig. 3-(b) (keeping in mind that exists a second such diagram). The contribution of this diagram to the retarded self-energy of the photon is [6, 21]:

$$\begin{aligned}-i\Pi^\mu{}_\mu(Q)|_R^{\text{self}} &= e^2 \int \frac{d^n R}{(2\pi)^n} \\ &\times \left\{ \left[ \frac{1}{2} - n_F(p_0) \right] [S_R(P) - S_A(P)] [S_R(R)]^2 \text{Tr}\boldsymbol{\Sigma}_R \right. \\ &\left. + \left[ \frac{1}{2} - n_F(r_0) \right] [S_R^2(R) \text{Tr}\boldsymbol{\Sigma}_R - S_A^2(R) \text{Tr}\boldsymbol{\Sigma}_A] S_A(P) \right\}\end{aligned}\quad (22)$$



where the notation  $\text{Tr}\Sigma_\alpha$  with  $\alpha = R, A$  stands for:

$$\text{Tr}\Sigma_\alpha \equiv \text{Tr} (\gamma_\mu \hat{R} [-i\Sigma_\alpha(R)] \hat{R} \gamma^\mu \hat{P}). \quad (23)$$

A similar relation is easily derived for the advanced self-energy. The one-loop fermion self-energy  $\Sigma_\alpha(R)$  is calculated in a covariant gauge with the effective soft gluon propagator of Eq. (9). The thermal distributions can be arranged in a simple way in order to give:

$$\begin{aligned} \text{Im}\Pi^\mu{}_\mu(Q)^{\text{self}} &= \frac{1}{2}e^2g^2 \int \frac{d^n R}{(2\pi)^n} [n_F(r_0) - n_F(p_0)] \\ &\times \int \frac{d^n L}{(2\pi)^n} [\Delta_R^{T,L,G}(L) - \Delta_A^{T,L,G}(L)] P_{T,L,G}^{\rho\sigma}(L) \text{Tr}_{\rho\sigma}^{\text{self}} \\ &\times [S_R(P) - S_A(P)] [S_R(R+L) - S_A(R+L)] \\ &\times [n_B(l_0) + n_F(r_0 + l_0)] \mathcal{P} \left( \frac{1}{(R^2 - M_\infty^2)^2} \right) \end{aligned} \quad (24)$$

for the transverse ( $T$ ), longitudinal ( $L$ ), and gauge ( $G$ ) contributions corresponding to the propagator of Eq. (9), where  $\mathcal{P}$  denotes the principal value and  $\text{Tr}_{\rho\sigma}^{\text{self}}$  stands for the Dirac's trace

$$\text{Tr}_{\rho\sigma}^{\text{self}} \equiv \text{Tr} [\gamma^\mu \hat{R} \gamma_\sigma (\hat{R} + \hat{L}) \gamma_\rho \hat{R} \gamma_\mu \hat{P}]. \quad (25)$$

The reason why we kept only the cut ( $b$ ) of Fig. 3-(b) is that when  $Q^2 \geq 0$  (which is the case of interest if one wants to study the production rate of real photons or of dileptons), the cuts ( $a$ ) and ( $c$ ) are not allowed by kinematical constraints. Indeed, an on-shell fermion can emit by bremsstrahlung only photons with a virtuality  $Q^2 < 0$ .

The same kind of calculations can be carried out for the contribution of the vertex correction of Fig. 3-(a) to the retarded self-energy of the photon [21, 6]:

$$\begin{aligned} -i\Pi^\mu{}_\mu(Q)|_R^{\text{vertex}} &= e^2 \int \frac{d^n R}{(2\pi)^n} P_{T,L,G}^{\rho\sigma}(L) \text{Tr}_{\rho\sigma}^{\text{vertex}} \\ &\times \left\{ \left[ \frac{1}{2} - n_F(p_0) \right] \left( V_{RRA}^{T,L,G}(P, Q, -R) S_R(P) - V_{ARA}^{T,L,G}(P, Q, -R) S_A(P) \right) S_R(R) \right. \\ &\left. + \left[ \frac{1}{2} - n_F(r_0) \right] \left( V_{ARA}^{T,L,G}(P, Q, -R) S_R(R) - V_{ARR}^{T,L,G}(P, Q, -R) S_A(R) \right) S_A(P) \right\} \end{aligned} \quad (26)$$

again corresponding to the transverse ( $T$ ), longitudinal ( $L$ ), and gauge ( $G$ ) terms of Eq. (9), where  $\text{Tr}_{\rho\sigma}^{\text{vertex}}$  contains the Dirac's algebra factors:

$$\text{Tr}_{\rho\sigma}^{\text{vertex}} \equiv \text{Tr} [\gamma_\mu \hat{R} \gamma_\rho (\hat{R} + \hat{L}) \gamma^\mu (\hat{P} + \hat{L}) \gamma_\sigma \hat{P}] \quad (27)$$

and the functions  $V_{\alpha\beta\gamma}^{T,L,G}(P, Q, -R)$  are the scalar part of the one loop  $q - q - \gamma$  vertex, where the gluon line of the loop is made of an effective propagator. These are equal to

$$\begin{aligned} V_{\alpha\beta\gamma}^{T,L,G}(P, Q, -R) &= -g^2 \int \frac{d^n L}{(2\pi)^n} \\ &\times \left\{ \left( \frac{1}{2} + n_B(l_0) \right) \left[ \Delta_R^{T,L,G}(L) - \Delta_A^{T,L,G}(L) \right] S_\alpha(P+L) S_\gamma(R+L) \right. \end{aligned}$$

$$\begin{aligned}
& + \left( \frac{1}{2} - n_F(r_0 + l_0) \right) [S_R(R+L) - S_A(R+L)] S_{\bar{\beta}}(P+L) \Delta_{\gamma}^{T,L,G}(L) \\
& + \left( \frac{1}{2} - n_F(p_0 + l_0) \right) [S_R(P+L) - S_A(P+L)] S_{\beta}(R+L) \Delta_{\bar{\alpha}}^{T,L,G}(L) \Big\}. \tag{28}
\end{aligned}$$

Inserting this expression into Eq. (26), and calculating in the same way the advanced self-energy, one obtains the contribution of Fig. 3-(a) to the imaginary part of the photon self-energy:

$$\begin{aligned}
\text{Im } \Pi^{\mu}_{\mu}(Q)^{\text{vertex}} &= \frac{1}{2} e^2 g^2 \int \frac{d^n R}{(2\pi)^n} [n_F(r_0) - n_F(p_0)] \\
&\times \int \frac{d^n L}{(2\pi)^n} \left[ \Delta_R^{T,L,G}(L) - \Delta_A^{T,L,G}(L) \right] P_{T,L,G}^{\rho\sigma}(L) \text{Tr}_{\rho\sigma}^{\text{vertex}} \\
&\times \left\{ [S_R(P) - S_A(P)] [S_R(R+L) - S_A(R+L)] \right. \\
&\times [n_B(l_0) + n_F(r_0 + l_0)] \mathcal{P} \left( \frac{1}{R^2 - M_{\infty}^2} \right) \mathcal{P} \left( \frac{1}{(P+L)^2 - M_{\infty}^2} \right) \\
&+ [S_R(R) - S_A(R)] [S_R(P+L) - S_A(P+L)] \\
&\left. \times [n_B(l_0) + n_F(p_0 + l_0)] \mathcal{P} \left( \frac{1}{P^2 - M_{\infty}^2} \right) \mathcal{P} \left( \frac{1}{(R+L)^2 - M_{\infty}^2} \right) \right\} \tag{29}
\end{aligned}$$

For the same kinematical reasons as in the self-energy diagram, the cuts (a) and (c) do not contribute to the production rate of real photons or lepton pairs. We notice at this point a high symmetry between the self-energy correction and the vertex correction. Two kind of terms appear in the latter and can be interpreted in terms of cut diagrams: the first term in the curly brackets above corresponds to cut (b) and is to be combined with Eq. (24) while the second term should be combined with the other self-energy correction mentioned above but not made explicit. Both classes of terms give identical contributions to the photon production rate, so that in the following we consider only the first term of Eq. (29) and Eq. (24), and take the other terms into account simply by multiplying by an overall factor 2.

### 3.3 Reduction of the traces

In order to make some simplifications more obvious, it is useful to compute the Dirac's traces  $\text{Tr}_{\rho\sigma}^{\text{self}}$  and  $\text{Tr}_{\rho\sigma}^{\text{vertex}}$  in such a way that the invariants  $P^2$ ,  $R^2$ ,  $(P+L)^2$  and  $(R+L)^2$  appear whenever possible. We get:

$$\text{Tr}_{\rho\sigma}^{\text{self}} = -4 \left[ 4R^2 Q_{\rho} R_{\sigma} - 4Q^2 R_{\rho} R_{\sigma} - g_{\rho\sigma} \left( R^2(R^2 - Q^2) + 2R^2 Q \cdot L - 2Q^2 R \cdot L \right) \right] \tag{30}$$

and

$$\begin{aligned}
\text{Tr}_{\rho\sigma}^{\text{vertex}} &= -4 \left[ 2(R^2 + (R+L)^2) P_{\rho} Q_{\sigma} - 2(P^2 + (P+L)^2) R_{\rho} Q_{\sigma} \right. \\
&\quad + 2L^2 (R_{\rho} R_{\sigma} + P_{\rho} P_{\sigma}) - 4Q^2 R_{\rho} P_{\sigma} \\
&\quad + g_{\rho\sigma} \left( P^2 R^2 + (P+L)^2 (R+L)^2 \right. \\
&\quad \left. \left. - L^2 (P^2 + R^2 + (P+L)^2 + (R+L)^2 - Q^2 - L^2) \right) \right]. \tag{31}
\end{aligned}$$

At this point, it is worth noting that we dropped terms proportional to  $L_\rho$  or  $L_\sigma$ , since they will disappear in the contraction with the projectors  $P_{T,L}^{\rho\sigma}$ :

$$L_\rho P_{T,L}^{\rho\sigma}(L) = 0. \quad (32)$$

Therefore, the expressions obtained above for the Dirac's traces should not be used to compute the gauge dependence of the production rate, since  $L_\rho P_G^{\rho\sigma}(L) \neq 0$ . In order to verify the independence of this rate with respect to the gauge parameter  $\xi$ , it is simpler to go back to the original expressions Eqs. (24), (29) and show a compensation of the gauge dependence between the self-energy and the vertex contributions, exactly in the same manner as at  $T = 0$ .

### 3.4 Kinematics

We now take into account the constraints provided by the discontinuities:

$$\begin{aligned} S_R(P) - S_A(P) &= 2\pi\epsilon(p_0)\delta(P^2 - M_\infty^2) \\ S_R(R+L) - S_A(R+L) &= 2\pi\epsilon(r_0 + l_0)\delta((R+L)^2 - M_\infty^2); \end{aligned} \quad (33)$$

this will enable us to perform two of the momentum integrals “for free”. Moreover, as already mentioned, the components of  $R$  and  $P$  are considered to be hard, whereas the components of  $Q$  and  $L$  are considered to be much smaller than the temperature  $T$ . Therefore,  $p_0$  and  $r_0 + l_0$  are of the same sign:

$$\epsilon(p_0)\epsilon(r_0 + l_0) = 1. \quad (34)$$

From the constraint  $\delta(P^2 - M_\infty^2)$ , we extract the value of  $r_0$ :

$$\begin{aligned} r_0 &= q_0 \pm \sqrt{r^2 - 2qr \cos \theta + q^2 + M_\infty^2} \\ &\approx q_0 \pm \left[ r - q \cos \theta + \frac{q^2}{2r}(1 - \cos^2 \theta) + \frac{M_\infty^2}{2r} \right], \end{aligned} \quad (35)$$

where  $\theta$  is the angle between the spatial components of  $R$  and  $Q$ . Since the possible two signs for  $r_0$  lead at the end to equivalent contributions, we will consider only the positive solution for  $r_0$ , and multiply when necessary the result by a factor 2 to take into account the other solution. From the constraint  $\delta((R+L)^2 - M_\infty^2)$ , we obtain the value of  $\cos \theta'$ , where  $\theta'$  is the angle between the spatial components of  $R$  and  $L$ :

$$\begin{aligned} \cos \theta' &= \frac{(r_0 + l_0)^2 - (r^2 + l^2 + M_\infty^2)}{2rl} \\ &\approx \frac{l_0}{l} + \frac{q_0 - q \cos \theta}{l}. \end{aligned} \quad (36)$$

Moreover, we must impose  $\cos \theta'$  to be in  $[-1, 1]$ , which can give additional constraints between  $l_0, l, q_0, q$  and  $\cos \theta$ . When needed, the variable  $\cos \theta''$ , where  $\theta''$  is the angle between  $Q$  and  $L$ , will be obtained by:

$$\cos \theta'' = \cos \theta \cos \theta' + \sin \theta \sin \theta' \cos \phi, \quad (37)$$

where  $\phi$  is the angle between the projections of  $Q$  and  $L$  on the plane defining the spherical coordinates basis. Given these relations, the angular variables we choose as independent ones are  $\theta$  and  $\phi$ ,  $\theta'$  being extracted from the constraint Eq. (36) and  $\theta''$  being given by Eq. (37).

With such a choice of independent variables, we can calculate approximate values for the various denominators entering the rate:

$$R^2 - M_\infty^2 = 2Q \cdot R - Q^2 \approx 2q_0 r \left[ 1 - \cos \theta + \frac{M_\infty^2}{2r^2} + \frac{Q^2}{2q_0^2} \right], \quad (38)$$

$$\begin{aligned} \int_0^{2\pi} \frac{d\phi}{(P+L)^2 - M_\infty^2} &= \int_0^{2\pi} \frac{d\phi}{Q^2 - 2Q \cdot R - 2Q \cdot L} \\ &\approx \frac{2\pi}{2q_0 r \left[ \left( 1 - \cos \theta + \frac{M_\infty^2}{2r^2} + \frac{Q^2}{2q_0^2} + \frac{L^2}{2r^2} \right)^2 - \frac{L^2}{r^2} \left( \frac{M_\infty^2}{r^2} + \frac{Q^2}{q_0^2} \right) \right]^{1/2}}, \end{aligned} \quad (39)$$

(the reason why we performed the integration over  $\phi$  at this point is that at the dominant order  $(P+L)^2 - M_\infty^2$  is the only quantity in which  $\phi$  appears).

It is worth noticing that with  $M_\infty = 0$  and  $Q^2 = 0$ , the denominator  $R^2 - M_\infty^2$  exhibits a collinear singularity when  $\theta = 0$ , *i.e.* when the photon is emitted collinearly to the hard fermion. Looking at the previous expressions, we see that it is natural to introduce the new variables:

$$\begin{aligned} u &\equiv 1 - \cos \theta \\ M_{\text{eff}}^2 &\equiv M_\infty^2 + \frac{Q^2 r^2}{q_0^2}. \end{aligned} \quad (40)$$

It is now clear that the collinear divergence is regulated by the effective fermion mass  $M_{\text{eff}}$  which acts as a cut-off in the integral over  $u$ . Therefore, the order of the result depends on the order of this cut-off, a question which will be discussed in the following paragraph.

### 3.5 Enhancement mechanism

*A priori*, we are faced with four kinds of angular integrals over the variable  $u$ :

$$\begin{aligned} I_1 &\equiv \int_0^2 \frac{du}{R^2 - M_\infty^2}, & I_2 &\equiv \int_0^2 \frac{du}{(P+L)^2 - M_\infty^2}, \\ I_3 &\equiv \int_0^2 \frac{du}{(R^2 - M_\infty^2)^2}, & I_4 &\equiv \int_0^2 \frac{du}{(R^2 - M_\infty^2)((P+L)^2 - M_\infty^2)}. \end{aligned} \quad (41)$$

Since the order of  $R^2 - M_\infty^2$  or  $(P+L)^2 - M_\infty^2$  is  $q_0 r$ , the orders we expect naïvely for these integrals are:

$$\begin{aligned} I_1, I_2 &= \mathcal{O}\left(\frac{1}{q_0 r}\right) \\ I_3, I_4 &= \mathcal{O}\left(\frac{1}{(q_0 r)^2}\right); \end{aligned} \quad (42)$$

and this would be right, up to logarithmic factors, if the collinear singularities were really logarithmic in the four integrals. This is actually the case for  $I_1$  and  $I_2$  but obviously not for  $I_3$ , which exhibits a power-like collinear singularity. Looking at the form of  $R^2 - M_\infty^2$ , we have for the order of  $I_3$ :

$$I_3 = \mathcal{O}\left(\frac{1}{(q_0 r)^2} \frac{1}{u^*}\right), \quad (43)$$

where  $u^* \sim M_{\text{eff}}^2/r^2$ . Therefore, the actual order of  $I_3$  depends on the order of the physical cut-off in the  $u$  integral, this dependence being a power-like one instead of a logarithmic one. Moreover, this integral is enhanced with respect to its naïve order when  $u^* \ll 1$ , which occurs when the virtuality of the emitted photon is small.

As for  $I_4$ , since the hard momenta  $R$  and  $P + L$  only differ by soft quantities, the denominators  $R^2 - M_\infty^2$  and  $(P + L)^2 - M_\infty^2$  are zero almost simultaneously. Let us quantify more precisely this assertion; to explain roughly what happens in this case, it is sufficient to write  $R^2 - M_\infty^2 \sim q_0 r(u + u^*)$  and  $(P + L)^2 - M_\infty^2 \sim q_0 r(u + u^{*'})$ . Again, we have  $u^* \sim M_{\text{eff}}^2/r^2$ . Moreover,  $u^{*'} - u^*$  is independent of the value of  $M_{\text{eff}}^2/r^2$  and is of order  $L^2/r^2 \ll 1$ . Therefore, we get the following orders for the integral  $I_4$ :

$$\begin{aligned} \text{If } u^* \leq L^2/r^2 : \quad I_4 &= \mathcal{O}\left(\frac{1}{(q_0 r)^2} \frac{1}{u^{*'} - u^*}\right) \gg \frac{1}{(q_0 r)^2} \\ \text{If } u^* \gg L^2/r^2 : \quad I_4 &= \mathcal{O}\left(\frac{1}{(q_0 r)^2} \frac{1}{u^*}\right) \end{aligned} \quad (44)$$

Like  $I_3$ , this integral is enhanced when  $u^* \ll 1$ . The reason why  $I_4$  behaves much like  $I_3$  whereas  $I_4$  contains two simple poles instead of a double one in the case of  $I_3$  lies, of course, in the very close vicinity of these two poles. In fact, when  $u^*$  is smaller than the distance between the two poles, the order of the result is controlled by this separation which is of order  $L^2/r^2$ . On the contrary, when the regulator  $u^*$  is larger than this separation, everything happens as if we had a double pole.

Recalling now that the fermionic thermal mass  $M_\infty$  is of order  $gT$ , we should distinguish various cases according to the value of the virtuality  $Q^2$  (see Eq. (40)):

- (i)  $Q^2/q_0^2 \ll g^2$  : in this case, the virtuality of the emitted photon does not play any role, and can be completely neglected, since  $M_{\text{eff}} \approx M_\infty$ . This case will be studied first since it is the simplest one, and will provide a basis for the case where the virtuality can no longer be neglected. In this case, the integrals  $I_3$  and  $I_4$  are enhanced whereas  $I_1$  and  $I_2$  have their “normal” order, therefore we can neglect every occurrence of  $I_1$  or  $I_2$ .
- (ii)  $g^2 \leq Q^2/q_0^2 \ll 1$  : in this case, the virtuality must be taken into account since its effect is at least as important as the effect of the fermion thermal mass. We still have  $u^* \ll 1$ , so that the remark made in (i) on the enhancement of  $I_3$  and  $I_4$  remains true. This section will make an intensive use of the results obtained in the case (i).
- (iii)  $Q^2/q_0^2 \sim 1$  : here also, the virtuality of the photon plays an important role. Moreover, this case is very different from the previous two since none of the  $I_i$ 's is enhanced, and therefore all must be taken into account. Another reason why this case is very different lies in the fact that there is no more a hierarchy between the various powers of  $Q^2/q_0^2$ ; as a consequence, all the powers of this quantity should be kept in the expansion of the numerator.

It is interesting to compare the status of mass singularities in our calculation with results obtained in previous works. Collinear singularities and their cancelation have been studied in (non-resummed) perturbation theory at two-loop order in QED/QCD [32, 33] and three-loop order in the  $\lambda\phi^3$  model [34]: in all cases the problem considered was the decay rate of a heavy particle into massless particles and a complete cancelation of collinear singularities associated to the massless particle propagators was found when summing over real and virtual diagrams and over all thermal processes. The equivalent problem here is the case  $Q^2 \neq 0$  but  $M_\infty^2 = 0$  and indeed our expressions are regulated by the photon virtuality: in the R/A formalism there is no need to distinguish between “real” and “virtual” diagrams as they are all included in rather compact expressions (see *e.g.* Eq. (45) below). It is the masslessness of the “decaying” particle ( $Q^2 = 0$ ) which generates the collinear singularity of interest here as it would in the previous studies if we had let  $Q^2 \rightarrow 0$ : indeed the two-loop correction to the invariant rate  $R$  was found to be  $\sim e^2 g^2 T^2 \ln(T^2/Q^2)$  [35], which is indeed logarithmically divergent when the photon virtuality vanishes. This softer singularity (compared to the “power-like” divergence above) can be understood because no HTL resummation was performed on the gluon propagator ( $L^2 = 0$ ) and therefore no Landau damping was included.

## 4 Production of quasi real photons: $Q^2/q_0^2 \ll g^2$

Let us now specialize to the production rate of almost real photons, which corresponds to the case denoted by (i) at the end of the previous section. From a technical point of view, this case is the simplest one. Nevertheless, it will serve as a basis for the production rate of photons having a small virtuality, since this latter case will appear as a generalization of the present case.

### 4.1 Expression of $\text{Im}\Pi^\mu{}_\mu$

By using the fact that  $Q^2 = 0$  and the fact that  $P, R$  are hard and  $Q, L$  are much smaller than  $T$ , it is possible to greatly simplify the expression of the imaginary part of the photon self-energy. In particular, we get some partial cancelations between the contributions of the self-energy and of the vertex. The remaining dominant term is:

$$\begin{aligned} \text{Im}\Pi^\mu{}_\mu(Q) &\approx -8e^2g^2 \int \frac{d^n R}{(2\pi)^{n-1}} \int \frac{d^n L}{(2\pi)^{n-1}} q_0 n'_F(p_0) n_B(l_0) \rho_{T,L}(l, l_0) \\ &\times \epsilon(p_0) \epsilon(r_0 + l_0) \delta(P^2 - M_\infty^2) \delta\left[(R+L)^2 - M_\infty^2\right] \\ &\times (R_\rho R_\sigma + P_\rho P_\sigma) P_{T,L}^{\rho\sigma} \frac{L^2}{(R^2 - M_\infty^2)((P+L)^2 - M_\infty^2)}, \end{aligned} \quad (45)$$

where we took into account the fact that the integral  $I_4$  is enhanced. We have also simplified the statistical factor  $n_F(r_0) - n_F(p_0)$  to  $q_0 n'_F(p_0)$  which is justified within our kinematical approximation. The fact that the first non vanishing term in the numerator is proportional to  $L^2 \ll T^2$  shows clearly that  $\text{Im}\Pi^\mu{}_\mu(Q)$  is zero at the HTL order.

Using Eqs. (35), (36), the expansion of the terms appearing in the numerator gives

$$\begin{aligned} L^2(R_\rho R_\sigma + P_\rho P_\sigma)P_T^{\rho\sigma} &\approx 2\left(\frac{r}{l}\right)^2 (L^2)^2 \\ L^2(R_\rho R_\sigma + P_\rho P_\sigma)P_L^{\rho\sigma} &\approx -2\left(\frac{r}{l}\right)^2 (L^2)^2. \end{aligned} \quad (46)$$

Using now the constraint  $-1 \leq \cos \theta' \leq 1$  (Eq. (36)), we see that the gluon momentum  $L$  is constrained to satisfy  $l_0/l \in [-1, 1]$ , *i.e.*  $L^2 < 0$ . This means that the production rate of real photons is dominated by the exchange of a space-like gluon (*i.e.*, by the Landau damping part of the gluon spectral density). Eq. (45) can be then be put into the form

$$\begin{aligned} \text{Im } \Pi^\mu{}_\mu(Q) &\approx (-1)_T \frac{e^2 g^2}{8\pi^4} \frac{1}{q_0} \int_{r^*}^{\infty} dr n'_F(r) \int_0^{l^*} l^4 dl \int_{-1}^{+1} dx n_B(lx) \rho_{T,L}(l, lx) (1-x^2)^2 \\ &\quad \times \int_0^2 \frac{du}{\left[ u + \frac{M_\infty^2}{2r^2} \right] \left[ \left( u + \frac{M_\infty^2}{2r^2} + \frac{l^2(x^2-1)}{2r^2} \right)^2 + \frac{l^2(1-x^2)M_\infty^2}{r^4} \right]^{1/2}}, \end{aligned} \quad (47)$$

where we denoted  $x \equiv l_0/l$ , and where the symbol  $(-1)_T$  denotes an extra minus sign in the transverse contribution. We have introduced some cut-offs  $r^*$  and  $l^*$  at a scale intermediate between  $gT$  and  $T$ , since we *a priori* restricted  $r$  to be hard and  $l$  to be negligible in front of  $T$ . We will see later that these cut-offs can be taken respectively to 0 and  $+\infty$ , without modifying significantly the result.

An alternate expression for  $\text{Im } \Pi^\mu{}_\mu(Q)$ , which will be needed later, can be obtained in the following way. Using the  $\delta$ -function constraints one easily derives

$$\frac{1}{R^2 - M_\infty^2} \frac{1}{(P+L)^2 - M_\infty^2} = -\frac{1}{2Q \cdot L} \left( \frac{1}{R^2 - M_\infty^2} + \frac{1}{(P+L)^2 - M_\infty^2} \right). \quad (48)$$

Then, noticing that the change of variables  $P+L \rightarrow -R$  leaves the integrand in Eq. (45) invariant it is legitimate to replace in this equation  $[(R^2 - M_\infty^2)((P+L)^2 - M_\infty^2)]^{-1}$  by  $[-Q \cdot L(R^2 - M_\infty^2)]^{-1}$ . We are then lead to the expression <sup>a</sup>

$$\begin{aligned} \text{Im } \Pi^\mu{}_\mu(Q) &\approx (-1)_T \frac{e^2 g^2}{2\pi^4} \frac{1}{q_0} \int_{r^*}^{\infty} r^2 dr n'_F(r) \\ &\quad \times \int_0^{l^*} l^4 dl \int_{-1}^{+1} dx n_B(lx) \rho_{T,L}(l, lx) (1-x^2)^2 \int_0^1 \frac{du'}{\sqrt{1-u'}} \frac{1}{4M_\infty^2 + l^2(1-x^2)u'}, \end{aligned} \quad (50)$$

---

<sup>a</sup>An alternative method to obtain the same result directly from Eq. (47) is to perform a few changes of variables:

$$\begin{aligned} u &\equiv \frac{lM_\infty}{r^2} \sqrt{1-x^2}t + \frac{l^2(1-x^2)}{2r^2} - \frac{M_\infty^2}{2r^2} \\ t &\equiv \frac{1}{2} \left( \frac{\alpha_0}{\alpha} - \frac{\alpha}{\alpha_0} \right) \quad \text{with} \quad \alpha_0 \equiv \frac{M_\infty}{l\sqrt{1-x^2}} \\ \alpha &\equiv \frac{1 - \sqrt{1-u'}}{2}. \end{aligned} \quad (49)$$

where the relation between the  $u'$  and  $u$  integration variables is  $u' \equiv -8r^2u/L^2$ .

## 4.2 Reduction of the expression

The expression of Eq. (50) can be simplified by performing the angular integration over the variable  $u'$ . This integral is elementary and gives:

$$\int_0^1 \frac{du'}{\sqrt{1-u'}} \frac{1}{4M_\infty^2 + l^2(1-x^2)u'} = 2 \frac{\tanh^{-1} \sqrt{-L^2/(4M_\infty^2 - L^2)}}{\sqrt{-L^2(4M_\infty^2 - L^2)}}. \quad (51)$$

At this point, we notice that the integral over  $r$  can now be factorized in order to obtain:

$$\int_{r^*}^{+\infty} dr r^2 n'_F(r) \approx \int_0^{+\infty} dr r^2 n'_F(r) = -\frac{\pi^2 T^2}{6}. \quad (52)$$

The reason why we can set the cut-off  $r^*$  to zero lies in the fact that the function to be integrated is peaked around  $r \sim T$ , whereas  $r^* \ll T$ . Indeed:

$$\int_0^{r^*} dr r^2 n'_F(r) \approx -\frac{(r^*)^3}{12T}. \quad (53)$$

Moreover, in order to further simplify the result, we will approximate the Bose-Einstein weight by  $n_B(lx) \approx T/lx$  since the momentum  $l$  is assumed to be much less than  $T$ .

Finally, if we recall that the spectral density to be used here is given by Eq. (14) since  $L^2 < 0$ , and if we introduce some convenient dimensionless quantities:

$$\begin{aligned} w &\equiv \frac{-L^2}{M_\infty^2} \\ \tilde{I}_{T,L}(x) &\equiv \frac{\text{Im} \Pi_{T,L}(x)}{M_\infty^2} \\ \tilde{R}_{T,L}(x) &\equiv \frac{\text{Re} \Pi_{T,L}(x)}{M_\infty^2}, \end{aligned} \quad (54)$$

the imaginary part of the real photon self-energy can be written as:

$$\begin{aligned} \text{Im} \Pi^\mu{}_\mu(Q) &\approx (-1)_T \frac{e^2 g^2 N_c C_F T^3}{3\pi^2 q_0} \int_0^1 \frac{dx}{x} \tilde{I}_{T,L}(x) \\ &\times \int_0^{w^*} dw \frac{\sqrt{w/(w+4)} \tanh^{-1} \sqrt{w/(w+4)}}{(w + \tilde{R}_{T,L}(x))^2 + (\tilde{I}_{T,L}(x))^2}, \end{aligned} \quad (55)$$

where we have re-introduced the required color and group factors.



### 4.3 Reduction using sum rules

Instead of performing first the angular integral over  $u$  to reduce Eq. (47) to the two-dimensional result of Eq. (55), it is possible to use sum rules to obtain the result as a one-dimensional integral.

Let us first recall that sum rules come in this context from the spectral representation of the resummed propagator, which can be written for the scalar-like part of the gluon propagator as:

$$\frac{i}{l_0^2 - l^2 - \Pi_{T,L}(l, l_0) + i\epsilon} = \int_{-\infty}^{+\infty} dE \frac{E}{2\pi} \rho_{T,L}(l, E) \frac{i}{l_0^2 - E^2 + i\epsilon}. \quad (56)$$

By taking the imaginary part of this equation, keeping in mind that  $\rho_{T,L}$  are real functions, we can then obtain:

$$\int_{-\infty}^{+\infty} \frac{dx}{2\pi} x \rho_{T,L}(l, lx) \mathcal{P} \left( \frac{1}{y^2 - x^2} \right) = \frac{l^2(y^2 - 1) - \text{Re}\Pi_{T,L}(y)}{\left( l^2(y^2 - 1) - \text{Re}\Pi_{T,L}(y) \right)^2 + \left( \text{Im}\Pi_{T,L}(y) \right)^2}, \quad (57)$$

where we denoted  $l_0 \equiv ly$  and  $E \equiv lx$ . By taking now special values of  $y$ , one easily obtains:

$$\begin{aligned} \text{With } y = 0 : \quad & \int_{-\infty}^{+\infty} \frac{dx}{2\pi} \frac{\rho_T(l, lx)}{x} = \frac{1}{l^2} \\ & \int_{-\infty}^{+\infty} \frac{dx}{2\pi} \frac{\rho_L(l, lx)}{x} = \frac{1}{l^2 + 3m_g^2} \\ \text{With } y = \infty : \quad & \int_{-\infty}^{+\infty} \frac{dx}{2\pi} x \rho_{T,L}(l, lx) = \frac{1}{l^2} \\ \text{With } |y| > 1 : \quad & \int_{-\infty}^{+\infty} \frac{dx}{2\pi} x \rho_{T,L}(l, lx) \mathcal{P} \left( \frac{1}{y^2 - x^2} \right) = \frac{1}{l^2(y^2 - 1) - \text{Re}\Pi_{T,L}(y)}. \end{aligned} \quad (58)$$

These are the basic sum rules we will use to perform the integral over  $x$ . However, the integrals we need to perform are on  $x \in [-1, +1]$  whereas the above sum rules give the result for an integration over the whole real axis. Therefore, it will be necessary to subtract the contributions of  $x \in ]-\infty, -1] \cup [1, +\infty[$ . This subtraction is easy to perform since in that region, the spectral functions  $\rho_{T,L}(l, lx)$  are made of delta functions corresponding to the thermal mass-shells of the gluon. More precisely, we have:

$$\int_{]-\infty, -1] \cup [1, +\infty[} \frac{dx}{2\pi} \rho_{T,L}(l, lx) f(x) = \frac{Z_{T,L}}{2l\omega_{T,L}} \left[ f \left( \frac{\omega_{T,L}}{l} \right) - f \left( -\frac{\omega_{T,L}}{l} \right) \right], \quad (59)$$

where  $Z_{T,L}$  stands for the residue of the spectral function on the mass-shell, whose energy is  $\omega_{T,L}(l)$ . Explicit forms of these residues can be found in Ref.[2]; for later use we record here the asymptotic limits

$$\omega_T^2(l \rightarrow \infty) \simeq l^2 + \frac{3}{2}m_g^2, \quad \omega_L^2(l \rightarrow \infty) \simeq l^2 \left[ 1 + 4 \exp \left( -\frac{2l^2}{3m_g^2} - 2 \right) \right],$$

$$\begin{aligned}
Z_T(l \rightarrow \infty) &\simeq 1 - \frac{3m_g^2}{4l^2} \ln \left( \frac{4l^2}{3m_g^2} \right), & Z_L(l \rightarrow \infty) &\simeq \frac{2l^2}{3m_g^2} \left[ 1 - \frac{4l^2}{m^2} \exp \left( -\frac{2l^2}{3m_g^2} - 2 \right) \right], \\
\omega_T^2(l \rightarrow 0) &\simeq m_g^2 + \frac{6}{5}l^2, & \omega_L^2(l \rightarrow 0) &\simeq m_g^2 + \frac{3}{5}l^2, \\
Z_T(l \rightarrow 0) &\simeq 1 - \frac{l^2}{5m_g^2}, & Z_L(l \rightarrow 0) &\simeq 1 + \frac{2l^2}{5m_g^2}.
\end{aligned} \tag{60}$$

As well, we can introduce in a natural way a magnetic mass for the transverse gluon by assuming that it modifies the static behavior in such a way that:

$$\Pi_T(0) = m_{\text{mag}}^2, \tag{61}$$

which, thanks to Eq. (57), is equivalent to:

$$\begin{aligned}
\int_{-\infty}^{+\infty} \frac{dx}{2\pi} x \rho_T(l, lx) &= \frac{1}{l^2}, \\
\int_{-\infty}^{+\infty} \frac{dx}{2\pi} \frac{\rho_T(l, lx)}{x} &= \frac{1}{l^2 + m_{\text{mag}}^2}.
\end{aligned} \tag{62}$$

These sum rules may now be used to reduce Eq. (50) down to a one-dimensional integral. To do this, we first cast Eq. (50) into the form

$$\begin{aligned}
\text{Im } \Pi^\mu{}_\mu(Q) &\approx (-1)_T \frac{e^2 g^2 T^3}{12\pi^2 q_0} \int_0^{l^*} l dl \int_{-1}^{+1} dx \rho_{T,L}(l, lx) \int_0^1 \frac{du'}{u' \sqrt{1-u'}} \times \\
&\frac{1}{2y^2} \left\{ \frac{2}{x} (x^2 - 1) + 2x(y^2 - 1) + (y^2 - 1)^2 \left[ \frac{1}{x+y} + \frac{1}{x-y} \right] \right\}
\end{aligned} \tag{63}$$

where  $y \equiv \sqrt{1 + 4M_\infty^2/l^2 u'}$ . The application of sum rules to evaluate Eq. (63) is now completely straightforward. We consider each of the terms in curly brackets in turn, and examine first of all the transverse contribution.

For the first term, we have a contribution due to

$$\begin{aligned}
K_1 &\equiv -2 \int_0^{l^*} l dl \int_{-1}^{+1} dx \rho_{T,L}(l, lx) \int_0^1 \frac{du'}{u' \sqrt{1-u'}} \frac{1}{2y^2} \frac{2}{x} (x^2 - 1) \\
&= \int_0^{l^*} \frac{dl}{\sqrt{l^2 + 4M_\infty^2}} \ln \left[ \frac{(l + \sqrt{l^2 + 4M_\infty^2})^2}{4M_\infty^2} \right] \left\{ (1 - Z_T) - l^2 \left( \frac{1}{l^2 + m_{\text{mag}}^2} - \frac{Z_T}{\omega_T^2} \right) \right\},
\end{aligned} \tag{64}$$

where we have introduced a magnetic mass  $m_{\text{mag}} \sim g^2 T$  via Eq. (62). Thanks to Eq. (60), this integral is finite for  $l \rightarrow 0$ , and in fact for  $M_\infty \sim gT$  we can drop  $m_{\text{mag}} \sim g^2 T$ , but not if  $M_\infty \sim g^2 T$  or below.

In the following we use the HTL result,  $M_\infty \sim gT$ , so that we can drop the dependence on the magnetic mass. It is also easy to see from Eq. (64) that since

$$m_g^2 \int_{l^*}^{\infty} \frac{dl}{l^3} \ln\left(\frac{l}{M_\infty}\right) \sim \left(\frac{m_g}{l^*}\right)^2 \ln\left(\frac{l^*}{M_\infty}\right), \quad (65)$$

we can take  $l^* \rightarrow \infty$  by introducing a negligible contribution.

For the remaining terms of Eq. (63), we find the sum rules lead to

$$\begin{aligned} K_2 &\equiv -2 \int_0^{l^*} l dl \int_{-1}^{+1} dx \rho_{T,L}(l, lx) \int_0^1 \frac{du'}{u' \sqrt{1-u'}} \frac{1}{2y^2} \left\{ 2x(y^2 - 1) + (y^2 - 1)^2 \left[ \frac{1}{x+y} + \frac{1}{x-y} \right] \right\}. \\ &= \int_0^{l^*} \frac{dl}{l} \int_0^1 \frac{du'}{\sqrt{1-u'}} \frac{4M_\infty^2}{4M_\infty^2 + l^2 u'} \left\{ Z_T \frac{\omega_T^2 - l^2}{4M_\infty^2 - u'(\omega_T^2 - l^2)} - \frac{\text{Re } \Pi_T(y)}{4M_\infty^2 - u' \text{Re } \Pi_T(y)} \right\}. \end{aligned} \quad (66)$$

We note that no magnetic mass term arises for this contribution. In this form, using Eqs. (60), it is straightforward to verify that Eq. (66) is finite as  $l \rightarrow 0$ , as there is a cancelation between the two terms in curly brackets. As well, as was the case of  $K_1$ , we can take the limit of the cutoff  $l^* \rightarrow \infty$  by introducing a negligible contribution. To carry out the  $u'$  integration in Eq. (66) it is convenient to add and subtract a term representing the small  $l$  behavior:

$$\begin{aligned} K_2 &= -2 \int_0^{\infty} \frac{dl}{l} \int_0^1 \frac{du'}{\sqrt{1-u'}} \frac{4M_\infty^2}{4M_\infty^2 + l^2 u'} \times \\ &\left\{ \left[ Z_T \frac{\omega_T^2 - l^2}{4M_\infty^2 - u'(\omega_T^2 - l^2)} - \frac{m_g^2}{4M_\infty^2 - m_g^2 u'} \right] - \left[ \frac{\text{Re } \Pi_T(y)}{4M_\infty^2 - u' \text{Re } \Pi_T(y)} - \frac{m_g^2}{4M_\infty^2 - m_g^2 u'} \right] \right\}. \end{aligned} \quad (67)$$

The integration over  $u'$  can now be carried out, but the explicit results depend on the signs of  $1 - 4M_\infty^2/\text{Re } \Pi_{T,L}(\chi)$ ,  $1 - 4M_\infty^2/(\omega_{T,L}^2 - l^2)$  and  $1 - 4M_\infty^2/m_g^2$ , where  $\chi = \sqrt{1 + 4M_\infty^2/l^2}$ . The quantity  $1 - 4M_\infty^2/\text{Re } \Pi_{T,L}(x)$  is plotted on Fig. 4, for both the transverse and longitudinal case. Since  $\omega_{T,L}^2 - l^2 = \text{Re } \Pi_{T,L}(x \equiv \omega_{T,L}/l)$ , and since  $\chi$  is varying from 1 to  $+\infty$ , these curves give us all the signs we need if we recall also the limits  $\lim_{x \rightarrow 1^+} 1 - 4M_\infty^2/\text{Re } \Pi_T(x) = 1 - 8M_\infty^2/3m_g^2$  and  $\lim_{x \rightarrow 1^+} 1 - 4M_\infty^2/\text{Re } \Pi_L(x) = -\infty$ . The case  $3/8 < M_\infty^2/m_g^2$  is the most interesting one physically (*e.g.*, an  $SU(3)$  gauge theory with less than 10 light flavors), and fortunately the simplest one. We find for the total transverse contribution the result:

$$\begin{aligned} \text{Im } \Pi^\mu{}_\mu(Q)|_T &\approx -\frac{e^2 g^2 T^3}{3\pi q_0} \int_0^{+\infty} \frac{dl}{l} \left\{ \frac{m_g^2}{l^2 + m_g^2} \frac{1}{\chi} \tanh^{-1} \frac{1}{\chi} \right. \\ &\left. + \frac{4M_\infty^2}{l^2 + 4M_\infty^2} \frac{1}{\sqrt{\frac{4M_\infty^2}{\text{Re } \Pi_T(\chi)} - 1}} \tan^{-1} \left( \frac{1}{\sqrt{\frac{4M_\infty^2}{\text{Re } \Pi_T(\chi)} - 1}} \right) \right\} \end{aligned}$$

$$\begin{aligned}
& -Z_T \frac{\omega_T^2 - l^2}{\omega_T^2} \frac{1}{\sqrt{\frac{4M_\infty^2}{\omega_T^2 - l^2} - 1}} \tan^{-1} \left( \frac{1}{\sqrt{\frac{4M_\infty^2}{\omega_T^2 - l^2} - 1}} \right) \\
& + \left( \frac{4M_\infty^2}{l^2 + 4M_\infty^2} - \frac{m_g^2}{l^2 + m_g^2} \right) \frac{1}{\sqrt{\frac{4M_\infty^2}{m_g^2} - 1}} \tan^{-1} \left( \frac{1}{\sqrt{\frac{4M_\infty^2}{m_g^2} - 1}} \right) \Bigg\}. \tag{68}
\end{aligned}$$

Likewise for the longitudinal case we obtain:

$$\begin{aligned}
\text{Im } \Pi^\mu{}_\mu(Q)|_L & \approx \frac{e^2 g^2 T^3}{3\pi q_0} \int_0^{+\infty} \frac{dl}{l} \left\{ \left( \frac{m_g^2}{l^2 + m_g^2} - \frac{3m_g^2}{l^2 + 3m_g^2} \right) \frac{1}{\chi} \tanh^{-1} \frac{1}{\chi} \right. \\
& + \frac{4M_\infty^2}{l^2 + 4M_\infty^2} \frac{1}{\sqrt{\frac{4M_\infty^2}{\text{Re}\Pi_L(x)} - 1}} \tan^{-1} \left( \frac{1}{\sqrt{\frac{4M_\infty^2}{\text{Re}\Pi_L(x)} - 1}} \right) \\
& - Z_L \frac{\omega_L^2 - l^2}{\omega_L^2} \frac{1}{\sqrt{\frac{4M_\infty^2}{\omega_L^2 - l^2} - 1}} \tan^{-1} \left( \frac{1}{\sqrt{\frac{4M_\infty^2}{\omega_L^2 - l^2} - 1}} \right) \\
& \left. + \left( \frac{4M_\infty^2}{l^2 + 4M_\infty^2} - \frac{m_g^2}{l^2 + m_g^2} \right) \frac{1}{\sqrt{\frac{4M_\infty^2}{m_g^2} - 1}} \tan^{-1} \left( \frac{1}{\sqrt{\frac{4M_\infty^2}{m_g^2} - 1}} \right) \right\}. \tag{69}
\end{aligned}$$

There are two other cases that need to be considered in general:  $1/4 < M_\infty^2/m_g^2 < 3/8$  and  $M_\infty^2/m_g^2 < 1/4$ . These two cases are more intricate because now the required signs depend on the value of  $l$ . For this reason, the corresponding expressions will not be written here. There is one limit of interest,  $M_\infty \rightarrow 0$ , which is included in the latter regime, but this limit is more conveniently handled at an earlier stage of the calculation (see Eq. (55)). One should note that this splitting in three ranges is only a consequence of the use of sum rules and has no physical meaning, since it is obvious from Eq. (50) that the result is a continuous function of the ratio  $M_\infty^2/m_g^2$ . The reason for this can be seen from Eq. (50): one must extend the  $x$  integration range from  $[-1, +1]$  to the whole real axis in order to use sum rules and then subtract the contribution of the region  $]-\infty, -1] \cup [+1, +\infty[$  by Eq. (59). While  $x \in [-1, +1]$ , the denominator  $4M_\infty^2 + l^2(1 - x^2)u'$  remains strictly positive; but if  $x \in ]-\infty, -1] \cup [+1, +\infty[$ , one can be faced with a pole in the  $u'$  variable, which is dealt with a principal part prescription. A by-product of this pole is that the expression that should be integrated over  $l$  depends on which side of the pole we are.

#### 4.4 Discussion of the result and asymptotic behavior

In this paragraph, we study the behavior of  $\text{Im} \Pi^\mu_\mu(Q)$  in some limiting cases for  $M_\infty^2$  and  $m_g^2$ . We work with the compact form Eq. (55). In fact, the quantity of interest is

$$J_{T,L} \equiv \int_0^1 \frac{dx}{x} \tilde{I}_{T,L}(x) \int_0^{w^*} dw \frac{\sqrt{w/(w+4)} \tanh^{-1} \sqrt{w/(w+4)}}{(w + \tilde{R}_{T,L}(x))^2 + (\tilde{I}_{T,L}(x))^2}, \quad (70)$$

which is dimensionless and is therefore a function of the dimensionless quantities  $l^*/M_\infty$  and  $m_g/M_\infty$ . The independence on  $l^*$ , as well as the infra-red finiteness, can be shown to hold using this formula, but since we already did this using the sum-rule formalism we will not repeat the discussion here. We thus assume  $J_{T,L}$  to be only a function of  $M_\infty/m_g$  and study, both analytically and numerically, the limit of the above expression when the ratio  $M_\infty/m_g \rightarrow 0$  in order to better understand the origin of the singularities. Of course, the precise value of this ratio is fixed by the number of colors and flavors of the studied theory, and is of order 1. Despite that fact, this limit enables one to verify what is the effect of switching the fermion thermal mass off, and gives information on the nature of the singularities which are regularized by this mass. Some details of the analysis are given in the appendix. We find:

$$\begin{aligned} J_L &\underset{M_\infty \ll m_g}{\sim} \ln \left( \frac{m_g}{M_\infty} \right) \\ J_T &\underset{M_\infty \ll m_g}{\sim} \ln^2 \left( \frac{m_g}{M_\infty} \right). \end{aligned} \quad (71)$$

These results are interpreted as follows: the thermal fermion mass regularizes the collinear divergence, and therefore this kind of divergence, common to both the longitudinal and the transverse cases, contributes as one power of  $\ln(m_g/M_\infty)$ . Additionally, in the transverse contribution, there is an extra power of that logarithm, which is a consequence of the potential infrared divergence due to the absence of a thermal mass for static transverse gluons. This means also that this divergence is unexpectedly regularized by the fermion thermal mass. In fact, we can see already these features in Eq. (51), where the  $\tanh^{-1}$  function corresponds to the collinear logarithmic factor and where the combination  $\sqrt{-L^2(4M_\infty^2 - L^2)}$  (instead of  $-L^2$  if  $M_\infty^2$  is not taken into account) in the denominator is responsible for the regularization of potential infrared problems. We can also observe in that limit the essential difference between a true double pole and the structure of the integral we denoted by  $I_4$  in the section 3.5 (indeed, as seen before,  $I_4$  is the integral of interest in our problem, because it is enhanced, and because it has the dominant part of the numerator associated with it). If we really had a double pole, like in  $I_3$ , we would have got a factor  $m_g^2/M_\infty^2$  instead of a logarithm. This point will be discussed further when we compare our results with that of [7, 8, 9]. We have checked that numerical calculations based on Eq. (70) are in good agreement with the analytical results in the asymptotic region.

In fact, if the fermion thermal mass is sufficiently small, there can be a competition between the fermion mass and an hypothetical magnetic mass, expected at the order  $m_{\text{mag}} \sim g^2 T$ . If we introduce this mass by the transformation of Eq. (61), then we obtain:

(i) If  $m_{\text{mag}} \ll M_\infty \ll m_g$ :

$$J_T \sim \ln^2 \left( \frac{m_g}{M_\infty} \right), \quad (72)$$

(ii) If  $M_\infty \ll m_{\text{mag}} \ll m_g$ :

$$J_T \sim \ln\left(\frac{m_g}{M_\infty}\right) \ln\left(\frac{m_g}{m_{\text{mag}}}\right). \quad (73)$$

This competition between the magnetic mass and the fermion mass has been studied numerically, which gives the curves of Fig. (5), where are plotted the value of  $J_T$  as a function of  $\log(m_{\text{mag}}/m_g)$ , for various fixed values of the ratio  $M_\infty/m_g$ . We observe that the effect of the magnetic mass becomes non negligible as far as  $m_{\text{mag}} \geq 0.1 M_\infty$ . When the magnetic mass is small enough, the flattening of the curves denotes the independence of the result on  $m_{\text{mag}}$ .

## 5 Comparison with the semi-classical results

The purpose of this section is to compare the results provided by the thermal field theory techniques with those obtained via semi-classical methods.

### 5.1 Structure of the emission rate

In the semi-classical approach, one finds [7, 8, 9, 36] that the emission rate of soft photons in a scattering process can be factorized as the product of two terms: the intensity of emission which is the square of an electromagnetic current, and the cross section for the same scattering process without photon emission. Our purpose is to make a precise connection between such a result and our result Eq. (45).

Let us begin by defining the amplitude corresponding to the scattering process without any photon emission, i.e. corresponding to the diagrams of Fig. 2-(d),(e) where the photon line is suppressed (written here for the scattering of a quark on another quark, but it is very simple to write it also for the scattering on a gluon; moreover, like in Eq. (45), we don't write the color and group factors):

$$\begin{aligned} i\mathcal{M}(P_1, P_2; P'_1, P'_2; L) &\equiv -\bar{u}(P'_1)(-ig\gamma^\mu)u(P_1) \bar{u}(P'_2)(-ig\gamma^\nu)u(P_2) \\ &\times \sum_{a=T,L} P_{\mu\nu}^a(L) \Delta^a(L), \end{aligned} \quad (74)$$

where  $P_1, P_2$  are the incoming momenta,  $P'_1, P'_2$  are the outgoing momenta, and  $L$  is the transferred momenta. Of course, only three of these five momenta are independent, and appropriate Dirac delta functions will be needed to enforce the momentum conservation. The amplitude squared is simply given by:

$$|\mathcal{M}|^2 = g^4 \text{Tr}(\gamma^\mu \not{P}_1 \gamma^\sigma \not{P}'_1) \text{Tr}(\gamma^\nu \not{P}_2 \gamma^\rho \not{P}'_2) \sum_{a,b=T,L} P_{\mu\nu}^a(L) P_{\rho\sigma}^b(L) \Delta^a(L) \left[ \Delta^b(L) \right]^*. \quad (75)$$

We are now going to rewrite Eq. 45 into a form exhibiting the decomposition mentioned above. In order to make the connection with Eq. 45, we first notice:

$$4(R_\rho R_\sigma + P_\rho P_\sigma) \approx \text{Tr}(\gamma^\rho (\not{R} + \not{L}) \gamma^\sigma \not{P}), \quad (76)$$

and

$$\frac{4e^2 L^2}{(R^2 - M_\infty^2)((P+L)^2 - M_\infty^2)} \approx -e^2 \sum_{\text{pol. } \varepsilon} \left( \frac{P \cdot \varepsilon}{P \cdot Q} - \frac{(R+L) \cdot \varepsilon}{(R+L) \cdot Q} \right)^2, \quad (77)$$

where the sum runs over the polarizations of the emitted photon. We recognize the standard electromagnetic current which appears in such a soft emission [36]. It is worth recalling that we used the fact that the relevant values of  $u$  are of order  $u^* \ll 1$ . We need also the hard thermal loop contribution to the imaginary part of the polarization tensor of the gluon:

$$\text{Im } \Pi_{\text{gluon}}^{\mu\nu}(L) = \frac{g^2}{2} \int \frac{d^4 K}{(2\pi)^4} [n_F(k_0 + l_0) - n_F(k_0)] \times \\ 2\pi\delta(K^2) 2\pi\delta((K + L)^2) \text{Tr}(\gamma^\mu \not{K} \gamma^\nu (\not{K} + \not{L})), \quad (78)$$

where we considered only the quark loop contribution. Of course, the gluon loop would be related to the scattering of the quark on a gluon, which has not been written. Moreover, like in Eq. (45) and Eq. (75), we have not written the color and group factors. Concerning the statistical weights of Eq. (45), a straightforward calculation gives (the  $n_B(q_0)$  factor should be added in order to reconstruct the emission rate defined in Eq. (4), and the other statistical factors have been taken at an earlier stage of the calculation, for example in Eqs. (24) and (29), before any approximation):

$$n_B(q_0) [n_B(l_0) + n_F(r_0 + l_0)] [n_F(r_0) - n_F(p_0)] [n_F(k_0 + l_0) - n_F(k_0)] \\ = n_F(r_0 + l_0) [1 - n_F(p_0)] n_F(k_0) [1 - n_F(k_0 + l_0)]. \quad (79)$$

We need also the following identity:

$$\text{Im } \Pi_{\text{gluon}}^{\nu\rho}(L) = \sum_{a,b=T,L} P_{\mu\nu}^a(L) P_{\rho\sigma}^b(L) {}^* \Delta^a(L) [{}^* \Delta^b(L)]^* \\ = - \sum_{a,b,c=T,L} \text{Im } \Pi_c(L) P_c^{\nu\rho}(L) P_{\mu\nu}^a(L) P_{\rho\sigma}^b(L) {}^* \Delta^a(L) [{}^* \Delta^b(L)]^* \\ = - \sum_{a=T,L} \text{Im } \Pi_a(L) |{}^* \Delta^a(L)|^2 P_{\mu\sigma}^a(L) \\ = -\frac{1}{2} \sum_{a=T,L} \rho_a(L) P_{\mu\sigma}^a(L), \quad (80)$$

the last equality being valid in the region where  $L^2 < 0$ .

Given all these relations, it is straightforward to rewrite our result for the emission rate (see Eqs. (4) and (45)) per unit time and unit volume as:

$$\frac{dN}{d^4x} \approx \frac{d^3q}{(2\pi)^3 2q_0} \int \prod_{i=1,2} \frac{d^4 P_i}{(2\pi)^4} \prod_{i=1,2} \frac{d^4 P'_i}{(2\pi)^4} (2\pi)^4 \delta(P_1 + P_2 - P'_1 - P'_2 - Q) \\ \times 2\pi n_F(p_1^0) \delta(P_1^2 - M_\infty^2) 2\pi [1 - n_F(p_1^0)] \delta(P_1'^2 - M_\infty^2) \\ \times 2\pi n_F(p_2^0) \delta(P_2^2) 2\pi [1 - n_F(p_2^0)] \delta(P_2'^2) \\ \times |\mathcal{M}|^2(P_1, P_2; P'_1 + Q, P'_2; L \equiv P'_2 - P_2) \\ \times e^2 \sum_{\text{pol. } \varepsilon} \left( \frac{P_1 \cdot \varepsilon}{P_1 \cdot Q} - \frac{P'_1 \cdot \varepsilon}{P'_1 \cdot Q} \right)^2, \quad (81)$$

where  $|\mathcal{M}|^2$  is given in Eq. (75). This expression shows clearly that thermal field theory calculation leads also to a separation in two factors: the amplitude squared of the similar scattering process without photon emission, and a factor which is nothing but the square of an electromagnetic current and is specific to the photon emission. These two factors are then integrated over the momenta of the unobserved particles, with appropriate statistical weights. Because of this high similarity with the semi-classical expressions, this structure can be seen as another evidence to say that the enhanced terms we have exhibited are actually the relevant contributions to photon production by a plasma.

This decomposition is valid only when the photon momentum  $Q$  is negligible in front of the quark momentum, so that the amplitude that appears in Eq. (81) is almost unperturbed by the momentum  $Q$ . It is worth saying that we used several times the fact that  $u^* \ll 1$  to give that structure to Eq. (45). It means that this kind of factorization will not be valid in the case where the virtuality is important  $Q^2/q_0^2 \sim 1$ . Moreover, compared to the standard semi-classical treatments [7, 8, 9], we see that this structure remains valid even if we take into account the transverse exchange contribution, which has been shown in the previous section to be of the same order of magnitude as the longitudinal one.

## 5.2 Factorization limit

Nevertheless, despite that nice structure, the phase space over which the integration has to be performed is common to the two factors. Indeed, these two factors share some variables, like the momentum  $L$  exchanged during the scattering. Therefore, from a technical point of view, the factorization is not really complete.

The integral over the angles  $\theta$  and  $\phi$  of the photon line affect only the factor related to the photon emission, and is easily obtained via Eqs. (77), (38), (39) and (51):

$$\int_0^{2\pi} d\phi \int_0^2 du \sum_{\text{pol. } \varepsilon} \left( \frac{P_1 \cdot \varepsilon}{P_1 \cdot Q} - \frac{P'_1 \cdot \varepsilon}{P'_1 \cdot Q} \right)^2 \approx \frac{16\pi}{q_0^2} \sqrt{\frac{-L^2}{4M_\infty^2 - L^2}} \tanh^{-1} \sqrt{\frac{-L^2}{4M_\infty^2 - L^2}}. \quad (82)$$

As already said, the  $\tanh^{-1}$  factor is a remnant of the collinear singularity (when  $M_\infty \rightarrow 0$ , this factor diverges logarithmically).

Then, we see that this emission factor still depends on the variable  $L^2$ , so that the apparent factorization provided by Eq. 81 is not a true factorization. We can look at the two limiting cases:

(i) If  $L \ll M_\infty$ , we have:

$$\int_0^{2\pi} d\phi \int_0^2 du \sum_{\text{pol. } \varepsilon} \left( \frac{P_1 \cdot \varepsilon}{P_1 \cdot Q} - \frac{P'_1 \cdot \varepsilon}{P'_1 \cdot Q} \right)^2 \approx \frac{-4\pi L^2}{q_0^2 M_\infty^2}. \quad (83)$$

Therefore, the coupling between  $L$  and  $M_\infty$  in the emission factor will be useful at small  $L$  to regularize potentially dangerous terms in the infrared sector. This is the reason why the transverse gluon exchange is infrared finite despite the lack of thermal mass for static transverse modes.

(ii) If  $L \gg M_\infty$ , we have:

$$\int_0^{2\pi} d\phi \int_0^2 du \sum_{\text{pol. } \varepsilon} \left( \frac{P_1 \cdot \varepsilon}{P_1 \cdot Q} - \frac{P'_1 \cdot \varepsilon}{P'_1 \cdot Q} \right)^2 \approx \frac{8\pi}{q_0^2} \ln \left( \frac{-L^2}{4M_\infty^2} \right). \quad (84)$$



This limit is known as the “factorization limit” [37]. Indeed, in that limit, the  $L$  dependence of the emission factor is only logarithmic and is therefore negligible, so that the only relevant  $L$  dependence is in the scattering amplitude.

This limit is valid for the longitudinal contribution when  $m_g \gg M_\infty$ , because in that case the relevant infrared regulator is  $m_g$  (which is the thermal mass of static longitudinal modes) and the relevant values of  $L$  are also of order  $L \sim m_g \gg M_\infty$ . In that limit, the longitudinal contribution becomes proportional to  $\ln(m_g^2/M_\infty^2)$ .

Almost the same interpretation can be given for the transverse contribution: we get one factor  $\ln(m_g^2/M_\infty^2)$  from the  $\tanh^{-1}$  when  $m_g \gg M_\infty$ , whereas the second power of that logarithm comes from the singular infrared behavior of the scattering amplitude. In that case, the “factorization limit” cannot be used for all the values of  $L$  since values of  $L$  of order  $M_\infty$  are explored due to the lack of transverse static thermal mass.

In conclusion, we can say that the expression Eq. (81), despite its high similarity with semi-classical ones, should be interpreted with care concerning the possibility of “factorization”. Moreover, this lack of factorization at small  $L$  is closely related to the possibility of getting a finite transverse contribution.

### 5.3 Order of magnitude

After having seen that our expression for the photon production rate, derived from thermal field theory, is similar to the expressions usually encountered in semi-classical methods, it remains to compare the order of magnitude of the rate given by the two methods since the calculations are performed in very different ways.

From Eq. (4) and the discussion in the previous section, the differential rate for real photon production, integrated over angular variables, takes the form

$$\frac{dN}{dq_0 d^4x} \approx \frac{e^2 g^2 N_C C_F}{6\pi^4} \frac{T^4}{q_0} (-1)_L J_{T,L} \left( \frac{m_g}{M_\infty} \right) \quad (85)$$

where one recognizes the typical  $1/q_0$  bremsstrahlung spectrum. It is instructive to compare our result with that in [7, 8, 9] in the case the LPM effect is turned off. It is found there, neglecting numerical constants, that in the semi-classical approximation

$$\frac{dN}{dq_0 d^4x} \approx e^2 g^4 \frac{T^6}{q_0 M_\infty^2} \ln \left( \frac{T^2}{m_g^2} \right). \quad (86)$$

The structure of this equation can be understood as follows: the  $T^2/M_\infty^2$  piece is arising from the collinear radiation of the photon by the hard quark, while the factor  $\ln(T^2/m_g^2)$  reflects the divergence of the quark scattering cross section in the plasma, screened by the Debye mass  $m_g$ . Eqs. (85) and (86) are in qualitative agreement since  $M_\infty^2 \sim g^2 T^2$  and both rates are of order  $e^2 g^2 T^4/q_0$ . In fact the enhancement mechanism discussed above is realized in [7, 8, 9] by the factor  $T^2/M_\infty^2$ . We interpret this pole in  $M_\infty^2$  as a use of the approximation of Eq. (83), extended to the region where  $L \sim T$  in order to get the logarithmic factor  $\ln(T^2/M_g^2)$ . This leads to a very different limiting behavior when  $M_\infty \rightarrow 0$  since in our approach we recover a logarithmic singularity while in the semi-classical approach one obtains a pole in  $M_\infty$  [9]. Another difference between Eq. (85) and the results of Cleymans *et al.* is

that the transverse gluon exchange gives a finite contribution which is equally important as that of the screened longitudinal one considered in [7, 8, 9]. As a consequence, the use of the static approximation to describe the interaction of the quark in the plasma is not justified in thermal field theory.

## 6 The slightly virtual case: $g^2 \leq Q^2/q_0^2 \ll 1$

We now consider the case (ii) of Sec. 3.5 where the virtuality  $Q^2$  is non negligible but remains small. This can be treated in a simple way thanks to the introduction of an effective fermion mass.

### 6.1 Expression of $\text{Im}\Pi^\mu{}_\mu$

As already mentioned, in this case we still have a clear hierarchy in the various powers of  $Q^2/q_0^2 \ll 1$ . The consequence of this hierarchy is that the dominant term of the numerator remains the same as in Eqs. (45), and that it can still be approximated by Eq. (46). In what concerns the denominators, we saw in Eqs. (38), (39) that their expression remains unchanged provided one replaces the fermion thermal mass  $M_\infty$  by an effective mass taking into account the effect of the virtuality of the emitted photon  $M_{\text{eff}}^2 \equiv M_\infty^2 + Q^2 r^2/q_0^2$ . Even before writing the expression of the imaginary part of the photon self-energy, we can notice that the positive virtuality  $Q^2 > 0$  has the consequence of increasing the effect of the fermion thermal mass. Another point to be looked at is the influence of the constraint  $\cos \theta' \in [-1, 1]$  on the phase space. By examining the denominators entering in the rate, we easily see that the relevant values of  $u$  in the integration over  $u$  are of order of  $u^* \sim M_{\text{eff}}^2/r^2$ . As far as  $Q^2/q_0^2 \ll 1$ , this collinear regulator is much smaller than 1. Therefore, we can still approximate  $\cos \theta' \approx l_0/l$ . Therefore, the effect of the constraint  $\cos \theta' \in [-1, 1]$  is still to confine  $L^2$  to negative values. Finally, in complete analogy with Eq. (47), the imaginary part of the self-energy of a virtual photon reads:

$$\begin{aligned} \text{Im}\Pi^\mu{}_\mu(Q) &\approx (-1)_T \frac{e^2 g^2}{8\pi^4} \frac{1}{q_0} \int_{r^*}^{\infty} dr n'_F(r) \int_0^{l^*} l^4 dl \int_{-1}^{+1} dx n_B(lx) \rho_{T,L}(l, lx) (1-x^2)^2 \\ &\times \int_0^2 \frac{du}{\left[ u + \frac{M_{\text{eff}}^2}{2r^2} \right] \left[ \left( u + \frac{M_{\text{eff}}^2}{2r^2} + \frac{l^2(x^2-1)}{2r^2} \right)^2 + \frac{l^2(1-x^2)M_{\text{eff}}^2}{r^4} \right]^{1/2}}, \end{aligned} \quad (87)$$

the notations being the same as in Eq. (47).

### 6.2 Reduction of the expression

The simplification of this imaginary part can be performed by the same tools as in Sec. 4.2. In particular, since the relevant values of the angular variable  $u$  are much smaller than one, the same approximations are valid. Despite that similarity, an essential difference lies in the fact that the integration over  $r$  cannot be factorized since the effective fermion mass now depends on  $r$ . If one introduces the dimensionless variables:

$$v \equiv \frac{r}{T}$$

$$\begin{aligned}
w &\equiv \frac{-L^2}{M_{\text{eff}}^2(v)} \\
\tilde{I}_{T,L}(x, v) &\equiv \frac{\text{Im} \Pi_{T,L}(x)}{M_{\text{eff}}^2(v)} \\
\tilde{R}_{T,L}(x, v) &\equiv \frac{\text{Re} \Pi_{T,L}(x)}{M_{\text{eff}}^2(v)},
\end{aligned} \tag{88}$$

Eq. (87) takes the form

$$\begin{aligned}
\text{Im} \Pi^\mu{}_\mu(Q) &\approx (-1)_T \frac{2e^2 g^2 N_C C_F T^3}{\pi^4 q_0} \int_{r^*/T}^{+\infty} dv v^2 \frac{1}{e^v + 1} \left[ 1 - \frac{1}{e^v + 1} \right] \\
&\times \int_0^1 \frac{dx}{x} \tilde{I}_{T,L}(x, v) \int_0^{w^*(v)} dw \frac{\sqrt{w/(w+4)} \tanh^{-1} \sqrt{w/(w+4)}}{(w + \tilde{R}_{T,L}(x, v))^2 + (\tilde{I}_{T,L}(x, v))^2}.
\end{aligned} \tag{89}$$

where, compared to Eq. (55), the integration over  $v$  cannot be factorized because of the  $v$  dependence contained in the quantities  $w^*$ ,  $\tilde{R}_{T,L}$  and  $\tilde{I}_{T,L}$ .

### 6.3 Discussion of the result

When the virtuality  $Q^2 > 0$  is switched on, the quantity which is worth studying is now the integral:

$$\begin{aligned}
J_{T,L} &\equiv \frac{6}{\pi^2} \int_{r^*/T}^{+\infty} dv v^2 \frac{1}{e^v + 1} \left[ 1 - \frac{1}{e^v + 1} \right] \int_0^1 \frac{dx}{x} \tilde{I}_{T,L}(x, v) \\
&\times \int_0^{w^*(v)} dw \frac{\sqrt{w/(w+4)} \tanh^{-1} \sqrt{w/(w+4)}}{(w + \tilde{R}_{T,L}(x, v))^2 + (\tilde{I}_{T,L}(x, v))^2},
\end{aligned} \tag{90}$$

where the explicit prefactor  $6/\pi^2$  is introduced to compare this definition for  $J_{T,L}$  with the previous one in the limit where  $Q^2 = 0$  and where the integral over  $v$  can be factorized.

*A priori*, the functions  $J_{T,L}$  depend of the four dimensionless quantities  $r^*/T$ ,  $l^*/M_\infty$ ,  $M_\infty/m_g$  and  $Q^2 T^2/q_0^2 m_g^2$ . Nevertheless, since the weight function  $p(v) \equiv v^2 e^v / (e^v + 1)^2$  is peaked around  $v \sim 1$ , the small values of  $v$  will be negligible in the result, which means that in fact this result does not depend on the value of the cut-off  $r^*$ , which thus can be taken to zero.

Another question which can be answered very simply by using the study done for the production of real photons concerns the absence of IR divergences when the emitted photon is virtual. Indeed, we saw earlier that the IR finiteness was in fact due to the presence of a fermion thermal mass. In the present case, the effect of this fermion mass is enhanced by the presence of a positive virtuality  $Q^2 > 0$ , since  $M_{\text{eff}} > M_\infty$ . Therefore, it is obvious that the production rate of virtual photons will be IR safe, even for the contribution of the transverse gluon, and without the need of a magnetic mass.

To end with generalities, one can notice that the functions  $J_{T,L}$  are decreasing functions of the virtuality  $Q^2$ . Indeed, if  $Q^2$  increases, the effective mass  $M_{\text{eff}}(r)$  increases uniformly in  $r$ . Then, according to the study performed in the case of real photons, the functions  $J_{T,L}$  should decrease.

Concerning the dependence on the UV cut-off  $l^*$ , one can evaluate the contribution of the region  $l \in [l^*, +\infty[$  as being:

$$\begin{aligned} J'_T &\approx \frac{9}{2\pi} \left(\frac{m_g}{l^*}\right)^2 \int_0^{+\infty} dv p(v) \ln\left(\frac{l^*}{M_{\text{eff}}(v)}\right) \\ J'_L &\approx -\frac{9}{\pi} \left(\frac{m_g}{l^*}\right)^2 \int_0^{+\infty} dv p(v) \ln\left(\frac{l^*}{M_{\text{eff}}(v)}\right). \end{aligned} \quad (91)$$

Neglecting the logarithms, the contribution of the hard region  $[l^*, +\infty[$  is of order  $(m_g/l^*)^2$ , and must be compared to  $J_{T,L}$  in order to know if we can make  $l^* = +\infty$ . If we recall that the values which contribute dominantly in the integral over  $v$  are of order 1, we see that the influence of the virtuality  $Q^2 > 0$  on  $J_{T,L}$  is controlled by the comparison of  $M_\infty^2$  and  $Q^2 T^2/q_0^2$  (see Eq. (40)). The results are as follows:

- (i) If  $Q^2/q_0^2 \ll M_\infty^2/T^2 \sim g^2$ , the virtuality  $Q^2$  has no effect and can be neglected: this case corresponds to the previous section. The functions  $J_{T,L}$  are of order 1, and the contribution of  $[l^*, +\infty[$  is negligible as far as  $l^* \gg m_g$ . It means that the hard region around  $l \sim T$  does not contribute.
- (ii) If  $Q^2/q_0^2 \sim g^2$ , we are in the intermediate region where the virtuality of the radiated photon and the fermion thermal mass have comparable effects. The functions  $J_{T,L}$  are still of order 1, and the conclusion of the previous case remains unchanged.
- (iii) If  $g^2 \ll Q^2/q_0^2$ , the effect of the virtuality becomes much more important than the effect of the fermion thermal mass  $M_\infty$ , so that  $M_{\text{eff}}^2 \approx Q^2 r^2/q_0^2$ . Moreover, in that case, we have  $m_g \ll M_{\text{eff}}(v \sim 1)$ . By using the same tools as in the previous section, one obtains easily the simplified expression:

$$J_{T,L}(l^* \rightarrow \infty) \approx \frac{3}{2\pi^2} \int_0^{+\infty} dv v^2 \frac{1}{e^v + 1} \left[1 - \frac{1}{e^v + 1}\right] \ln\left(\frac{M_{\text{eff}}^2(v)}{m_g^2}\right) \int_0^1 \frac{dx}{x} \tilde{I}_{T,L}(x, v) \quad (92)$$

and, separating the transverse and longitudinal terms, one gets:

$$\begin{aligned} J_T(l^* \rightarrow \infty) &\approx \frac{3}{8\pi} \frac{q_0^2 m_g^2}{Q^2 T^2} \ln\left(\frac{Q^2 T^2}{q_0^2 m_g^2}\right) \\ J_L(l^* \rightarrow \infty) &\approx -2J_T(l^* \rightarrow \infty), \end{aligned} \quad (93)$$

where the  $v$  dependence is neglected inside the logarithm. We have checked that this approximation is in agreement with numerical estimates of Eq. (90). We are now in position to compare the contribution from  $[l^*, +\infty[$  with that of  $[0, l^*]$ . To make the discussion more precise, let us assume that  $Q^2/q_0^2 = g^\alpha$  and  $l^* = g^\beta T$ , with  $\alpha, \beta > 0$ . Then, neglecting the logarithmic factors in our comparison, we have:

$$J'_{T,L} \ll J_{T,L}$$

$$\begin{aligned}
&\iff J'_{T,L} \ll J_{T,L}(l^* \rightarrow \infty) \\
&\iff g^\alpha \ll g^{2\beta} \\
&\iff \beta < \alpha/2 \quad \text{since } g \ll 1.
\end{aligned} \tag{94}$$

This means that for fixed  $Q^2/q_0^2 = g^\alpha \ll 1$ , the dependence on  $l^*$  disappears as long as  $l^* > g^\beta T$  with  $0 < \beta < \alpha/2$ , and so the contribution to the result of the region beyond such a  $l^*$  is negligible. Therefore, in the region which contributes dominantly to the result, we still have  $l \leq g^\beta T \ll T$ , since  $\beta > 0$ . This means that our kinematical approximations are safe. Of course, this works since we had  $Q^2/q_0^2 \ll 1$  so that  $\alpha$  is strictly positive. When the ratio  $Q^2/q_0^2$  approaches the value 1, the negligible region around  $l \sim T$  becomes smaller and smaller, so that the precision of our approximations decreases. Another way to say the same thing is that given a fixed value of  $g \ll 1$  and given an accuracy one wants to ensure, there exists an  $\alpha > 0$  so that  $Q^2/q_0^2$  must remain lower than  $g^\alpha$ . In order to reach values of  $Q^2/q_0^2$  closer to 1, one has to relax the constraint on the accuracy or to consider a smaller  $g$ . We emphasize that, although we have introduced here fractional powers of the coupling constant  $g$  in order to quantify when our approximations for evaluating the bremsstrahlung diagrams are valid, this does not mean that the perturbation expansion, in integer powers of  $g$ , breaks-down; nevertheless, before calculating next-to-leading order diagrams, one should improve the approximations for the leading ones.

A general consequence of this analysis is the fact that the relevant scales in our problem are not only  $gT$  and  $T$  like in the standard HTL framework, but also the scale of the effective mass  $M_{\text{eff}}(v \sim 1) \approx M_\infty^2 + Q^2 T^2/q_0^2$  which is intermediate between  $gT$  and  $T$ . This is a consequence of the fact that the regularization of all our divergences, including the infrared one, is done by this effective mass rather than by the resummation of the HTLs in the gluon propagator.

The case  $Q^2/q_0^2 \sim 1$  does not fit in these approximations since in that case  $\alpha$  is of order zero, so that  $\beta$  is also of order zero and even the hard values of  $l$  contributes to the result.

To summarize this section, the functions  $J_{T,L}$  have been plotted as a function of  $\log(Q^2/q_0^2)$  on Fig. 6 over the whole range of admissible values of  $Q^2$ . We observe a clear flattening of the curves for small enough  $Q^2/q_0^2$ , indicating that the dependence on  $Q^2$  becomes negligible. In the opposite direction, we see that the enhancement of the rate decreases if  $Q^2 \rightarrow q_0^2$ . The enhancement (ratio between the values of  $J_{T,L}$  at  $Q^2/q_0^2 = 0$  and at  $Q^2/q_0^2 \sim 1$ ) decreases also if the coupling constant  $g$  increases. We note also that the longitudinal and transverse contributions are almost equal in magnitude.

## 6.4 Reduction using sum rules

Again, it is possible to reduce Eq. (87) by performing exactly the integral over  $x$  thanks to sum rules. Since now we cannot factorize the integral over  $r$ , the result given by sum rules is a two-dimensional integral. The techniques to achieve that are exactly the same as in Sec. 4.3, and therefore will not be reproduced here. We still need to distinguish three cases. For example, for the phenomenologically relevant case,  $3/8 < M_\infty^2/m_g^2$ , the quantities  $1 - 4M_{\text{eff}}^2(r)/\text{Re}\Pi_{T,L}(\chi)$ ,  $1 - 4M_{\text{eff}}^2(r)/(\omega_{T,L}^2 - l^2)$  and

$1 - 4M_{\text{eff}}^2(r)/m_g^2$  are negative for every value of  $r$ . The integration over  $u'$  gives in the transverse case:

$$\begin{aligned}
\text{Im } \Pi^\mu{}_\mu(Q)|_T &\approx -\frac{2e^2 g^2 T^3}{\pi^3 q_0} \int_0^{+\infty} dv v^2 \frac{1}{e^v + 1} \left[ 1 - \frac{1}{e^v + 1} \right] \int_0^{+\infty} \frac{dl}{l} \left\{ \frac{m_g^2}{l^2 + m_g^2} \frac{1}{\chi} \tanh^{-1} \frac{1}{\chi} \right. \\
&\quad + \frac{4M_{\text{eff}}^2(v)}{l^2 + 4M_{\text{eff}}^2(v)} \frac{1}{\sqrt{\frac{4M_{\text{eff}}^2(v)}{\text{Re } \Pi_T(\chi)} - 1}} \tan^{-1} \left( \frac{1}{\sqrt{\frac{4M_{\text{eff}}^2(v)}{\text{Re } \Pi_T(\chi)} - 1}} \right) \\
&\quad - Z_T \frac{\omega_T^2 - l^2}{\omega_T^2} \frac{1}{\sqrt{\frac{4M_{\text{eff}}^2(v)}{\omega_T^2 - l^2} - 1}} \tan^{-1} \left( \frac{1}{\sqrt{\frac{4M_{\text{eff}}^2(v)}{\omega_T^2 - l^2} - 1}} \right) \\
&\quad \left. + \left( \frac{4M_{\text{eff}}^2(v)}{l^2 + 4M_{\text{eff}}^2(v)} - \frac{m_g^2}{l^2 + m_g^2} \right) \frac{1}{\sqrt{\frac{4M_{\text{eff}}^2(v)}{m_g^2} - 1}} \tan^{-1} \left( \frac{1}{\sqrt{\frac{4M_{\text{eff}}^2(v)}{m_g^2} - 1}} \right) \right\}. \quad (95)
\end{aligned}$$

For the other cases  $1/4 < M_\infty^2/m_g^2 < 3/8$  and  $M_\infty^2/m_g^2 < 1/4$  similar calculations can be carried out but they are much more complex since the signs which control the expressions depend on both  $v$  and  $l$ .

## 7 The case: $Q^2/q_0^2 \sim 1$

This case will not be studied in detail in this paper; we discuss only why it is very different from the previous ones, and what is the expected order of magnitude of the production rate. This case differs from the previous two in the following respects:

- (i) Since  $Q^2/q_0^2 \sim 1$ , all powers of this ratio should now be kept in the expansion of the quantities we need.
- (ii) The relevant values of the angular variable  $u$  are now of order  $u^* \sim 1$ . Therefore, the collinear approximation (which means keeping only the term in  $u^0$  in the numerator) cannot be used. For the same reason, the approximation  $\cos \theta' \approx l_0/l$  is no longer valid. This means that the contribution of the domain  $L^2 > 0$  is as important as the contribution of the Landau damping  $L^2 < 0$ . Physically, this corresponds to processes involving the Compton effect (a thermalized on-shell gluon is absorbed by the moving quark, which emits a photon).
- (iii) The scattering of the quark is now sensitive to parton exchanges of hard momentum. As a consequence, the approximation  $l_0, l \ll T$  cannot be used in this case. Moreover, since our argument to neglect the diagram of Fig. 1-(c) was essentially based on the possibility to neglect a Fermi-Dirac statistical weight in front of a Bose-Einstein one when  $l_0 \ll T$ , it is now impossible to apply it. Therefore, this diagram contributes now at the same order.

Extrapolations of the previous case (despite its incompleteness) based on Eqs. (93), as well as preliminary estimations of the order of magnitude for the production rate of a static photon ( $Q^2/q_0^2 =$

1), seems to indicate that the bremsstrahlung gives a contribution  $\text{Im} \Pi^\mu{}_\mu \sim e^2 g^4 T^3 / q_0$ . Therefore, the diagram of Fig. 1-(a), already considered by Braaten, Pisarski and Yuan, is not the only contribution to the production of virtual photons.

## 8 Summary

We have studied the production of photons of energy  $q_0 \ll T$  by a plasma. For virtualities verifying  $Q^2/q_0^2 \ll 1$ , this photon emission is dominated by the bremsstrahlung process. In this calculation of the photon production rate, the HTL framework appeared to be insufficient in two respects: first of all, the standard HTL power counting breaks down in extracting the dominant contributions to this rate. Indeed, the diagram we considered is supposed to be sub-dominant in the HTL expansion, but turns out to dominate over the diagrams considered in the HTL framework. The reason for this failure lies in a strong enhancement of our diagrams due to collinear sensitivity. Secondly, once the relevant contributions have been isolated, the HTL resummation of soft lines is insufficient to regularize collinear divergences. This problem is solved by the application of a recent extension of the HTL resummation program. The imaginary part of the polarization tensor we get, proportional to the production rate, goes from  $\text{Im} \Pi^\mu{}_\mu \sim e^2 g^2 T^3 / q_0$  when  $Q^2/q_0^2 \ll g^2$  to  $\text{Im} \Pi^\mu{}_\mu \sim e^2 g^4 T^3 / q_0$  when  $Q^2/q_0^2 \sim 1$ . At the same time, when the ratio  $Q^2/q_0^2$  increases, the bremsstrahlung process becomes more and more sensitive to gluon exchanges of momentum intermediate between the soft scale  $gT$  and the hard scale  $T$ , which is again an important qualitative difference with the standard HTL calculations.

When the virtuality  $Q^2/q_0^2$  approaches 1, the enhancement disappears, but the bremsstrahlung process remains of an order comparable to the contributions already calculated by Braaten, Pisarski and Yuan. This may be interpreted as follows: the rate obtained within the HTL expansion by BPY is unexpectedly subleading due to a partial cancelation when taking the trace  $\Pi^\mu{}_\mu$  of the polarization tensor  $\Pi^\mu{}_\nu$ . Therefore, other terms subleading in the HTL power counting rules may contribute as well.

## 9 Acknowledgments

One of us (EP) thanks F. Flechsig, A. Rebhan, and H. Schulz for valuable discussions. The work of PA and FG is supported in part by the EEC program ‘‘Human Capital and Mobility’’, Network ‘‘Physics at High Energy Colliders’’, contract CHRX-CT93-0357 (DG 12 COMA). The work of RK and EP is supported by the Natural Sciences and Engineering Research Council of Canada. We also acknowledge support by NATO under grant CRG. 930739.

## 10 Appendix

To discuss the asymptotic behavior of the integrals  $J_{T,L}$  defined in Eq. (70), it is convenient to split the integral over  $w$  in  $J_{T,L}$  in order to obtain:

$$J_{T,L} = \int_0^1 \frac{dx}{x} \tilde{I}_{T,L}(x) \left[ \int_0^1 dw \frac{\sqrt{w/(w+4)} \tanh^{-1} \sqrt{w/(w+4)}}{(w + \tilde{R}_{T,L}(x))^2 + (\tilde{I}_{T,L}(x))^2} \right]$$

$$+ \int_0^1 dw \frac{\sqrt{1/(1+4w)} \tanh^{-1} \sqrt{1/(1+4w)}}{(1+w\tilde{R}_{T,L}(x))^2 + (w\tilde{I}_{T,L}(x))^2}. \quad (96)$$

In each of the two terms, we will use the small  $w$  approximation:

$$\begin{aligned} \sqrt{w/(w+4)} \tanh^{-1} \sqrt{w/(w+4)} &\underset{w \ll 1}{\approx} \frac{w}{4} \\ \sqrt{1/(1+4w)} \tanh^{-1} \sqrt{1/(1+4w)} &\underset{w \ll 1}{\approx} \frac{\ln(1/w)}{2}. \end{aligned} \quad (97)$$

Moreover, since the dominant behavior of the integrals  $J_{T,L}$  is controlled by the small  $x$  region, we will use the following approximations

$$\begin{aligned} \tilde{R}_L(x) &\underset{x \ll 1}{\approx} \frac{3m_g^2}{M_\infty^2} & \tilde{I}_L(x) &\underset{x \ll 1}{\approx} -\frac{3m_g^2 x}{2M_\infty^2} \\ \tilde{R}_T(x) &\underset{x \ll 1}{\approx} \frac{3m_g^2 x^2}{2M_\infty^2} & \tilde{I}_T(x) &\underset{x \ll 1}{\approx} \frac{3m_g^2 x}{4M_\infty^2}. \end{aligned} \quad (98)$$

The only supplementary ingredient we need is to recall that the two functions  $\tilde{R}_{T,L}(x)$  and  $\tilde{I}_{T,L}(x)$  are proportional to the ratio  $m_g^2/M_\infty^2$ , which determines their order of magnitude, compared to  $w$  which is of order 1. After a bit of algebra, one obtains the Eqs. (71).

## References

- [1] R. Pisarski, *Physica* **A158**, 146, 246 (1989); *Phys. Rev. Lett.* **63**, 1129 (1989).
- [2] E. Braaten and R. D. Pisarski, *Nucl. Phys.* **B337**, 569 (1990); **B339**, 310 (1990).
- [3] J. Frenkel and J. C. Taylor, *Nucl. Phys.* **B334**, 199 (1990); *Z. Phys.* **C49**, 515 (1991).
- [4] E. Braaten, R. D. Pisarski and T. C. Yuan, *Phys. Rev. Lett.* **64**, 2242 (1990).
- [5] R. Baier, S. Peigné, and D. Schiff, *Z. Phys.* **C62**, 337 (1994).
- [6] P. Aurenche, T. Becherrawy, and E. Petitgirard, hep-ph/9403320 preprint (1993).
- [7] J. Cleymans, V. V. Goloviznin and K. Redlich, *Phys. Rev.* **D47**, 989 (1993).
- [8] J. Cleymans, V. V. Goloviznin and K. Redlich, *Z. Phys.* **C59**, 495 (1993).
- [9] V. V. Goloviznin and K. Redlich, *Phys. Lett.* **B319**, 520 (1993).
- [10] L. D. Landau and I. Ya. Pomeranchuk, *Dokl. Akad. Nauk* **92**, 535 (1953); **92**, 735 (1953); A.B. Migdal, *Phys. Rev.* **103**, 1811 (1956).
- [11] E. Quack and P. A. Henning, *Phys. Rev. Lett.* **75**, 2811 (1995); hep-ph/9508201 (to appear in *Phys. Rev. D*).



- [12] J. Knoll and D. N. Voskresensky, Phys. Lett. **B351**, 43 (1995); GSI-Preprint 95-63, hep-ph/9510417.
- [13] A. Weldon, Phys. Rev. **49**, 1579 (1994).
- [14] S. Gupta, D. Indumathi, P. Mathews and V. Ravindran, Nucl. Phys. **B4580**, 189 (1996).
- [15] P. Aurenche, F. Gelis, R. Kobes and E. Petitgirard, hep-ph/9604398 preprint (to be published in Phys. Rev. **D**).
- [16] A. Niegawa, Mod. Phys. Lett. **A9**, 355 (1995).
- [17] F. Flechsig and A. K. Rebhan, Nucl. Phys. **B464**, 279 (1996).
- [18] U. Krammer, A. K. Rebhan and H. Schulz, Phys. Rev. **D52**, 2994 (1995).
- [19] A. K. Rebhan, Nucl. Phys. **B430**, 319 (1994)
- [20] C. Gale and J.I. Kapusta, Nucl. Phys. **B357**, 65 (1991).
- [21] P. Aurenche and T. Becherrawy, Nucl. Phys. **B379**, 259 (1992).
- [22] C. M. A. van Eijck and Ch. G. van Weert, Phys. Lett. **B278**, 305 (1992).
- [23] C. M. A. van Eijck, Ch. G. van Weert, and R. Kobes, Phys. Rev. **D50**, 4097 (1994).
- [24] A. Fetter and J. Walecka, Quantum Theory of Many Particle Systems, Mc Graw and Hill.
- [25] A. Niemi and G.W. Semenoff, Ann. Phys. **152** (1984) 105; Nucl. Phys. **B230** (1984) 181.
- [26] R. Kobes and G.W. Semenoff, Nucl. Phys. **B260** (1985) 714; Nucl. Phys. **B272** (1986) 329.
- [27] N. P. Landsman and Ch. G. van Weert, Phys. Rep. **145** (1985) 141.
- [28] H. A. Weldon, Phys. Rev. **D26**, 1384, (1982).
- [29] V. V. Klimov, Sov. J. Nucl. Phys. **33**, 934 (1981);  
Sov. Phys. JETP **55**, 199 (1982).
- [30] R.D. Pisarski, Physica **A158**, 146 (1989).
- [31] H. A. Weldon, Phys. Rev. **D26**, 2789, (1982).
- [32] J. Cleymans and I. Dadic, Z. Phys. **C42**, 133 (1989).
- [33] R. Baier, B. Pire and D. Schiff, Phys. Rev. **D38**, 2814 (1988);  
T. Altherr, P. Aurenche and T. Becherrawy, Nucl. Phys. **B315**, 436 (1989);  
T. Altherr and T. Becherrawy, Nucl. Phys. **B330**, 174 (1990);  
Y. Gabellini, T. Grandou and D. Poizat, Ann. Phys. **202**, 436 (1990).
- [34] M. Le Bellac and P. Reynaud, Nucl. Phys. **B380**, 423 (1992).

- [35] T. Altherr and P. Aurenche, Z. Phys. **C45**, 99 (1990).
- [36] L.D. Landau, E.M. Lifchitz, Electrodynamique quantique, Chap. X (Cours de Physique Théorique, IV), Ed. MIR, Moscou, (1989).
- [37] S. Peigné, Thèse de l'Université de Paris-Sud, Orsay (1995).

## Figure Captions

Fig. 1 Contributions to the soft photon production rate with soft internal lines.

Fig. 2 a,b,c: matrix elements contributing to the imaginary part of diagrams (a) and (c) of the previous figure; d,e: matrix elements contributing to the imaginary part of the gluon tadpole diagram in Fig. 1.

Fig. 3 Contributions to the soft photon production rate with hard internal fermion lines – (a): vertex insertion; (b): self-energy insertion.

Fig. 4  $1 - 4M_\infty^2/\text{Re } \Pi_{T,L}(x)$ .

Fig. 5 Effect of the magnetic mass on  $J_T$ .

Fig. 6  $J_{T,L}$  as a function of  $\log(Q^2/q_0^2)$ .

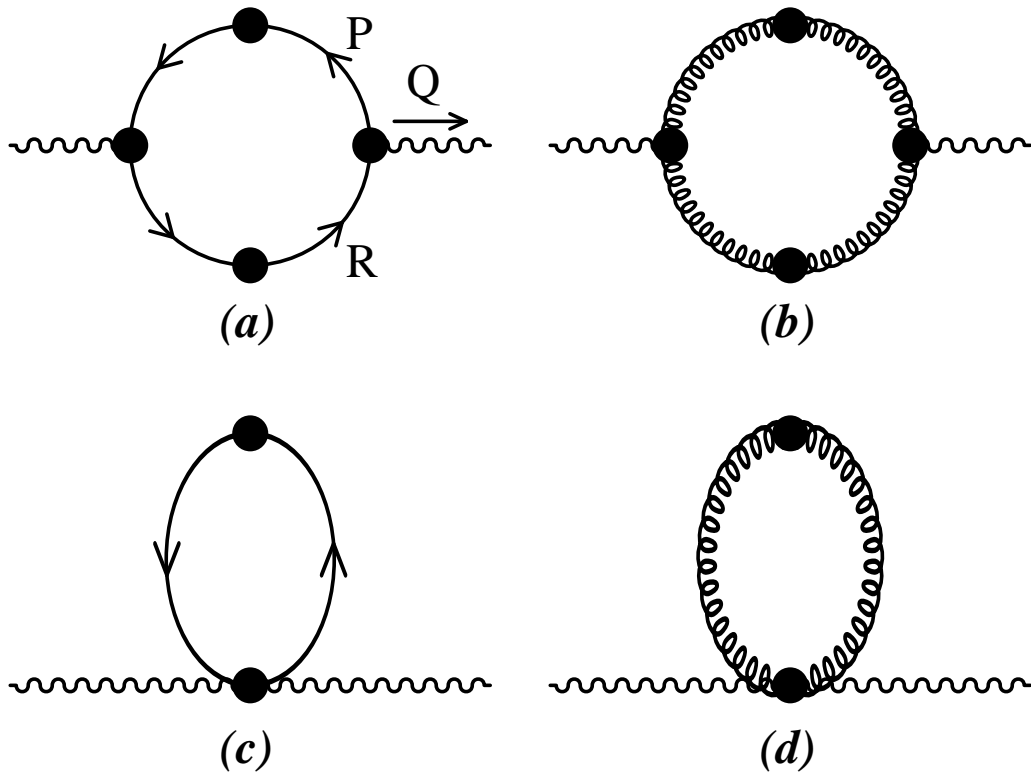


Figure 1: Contributions to the soft photon production rate with soft internal lines. The solid dots indicate effective propagators or vertices.

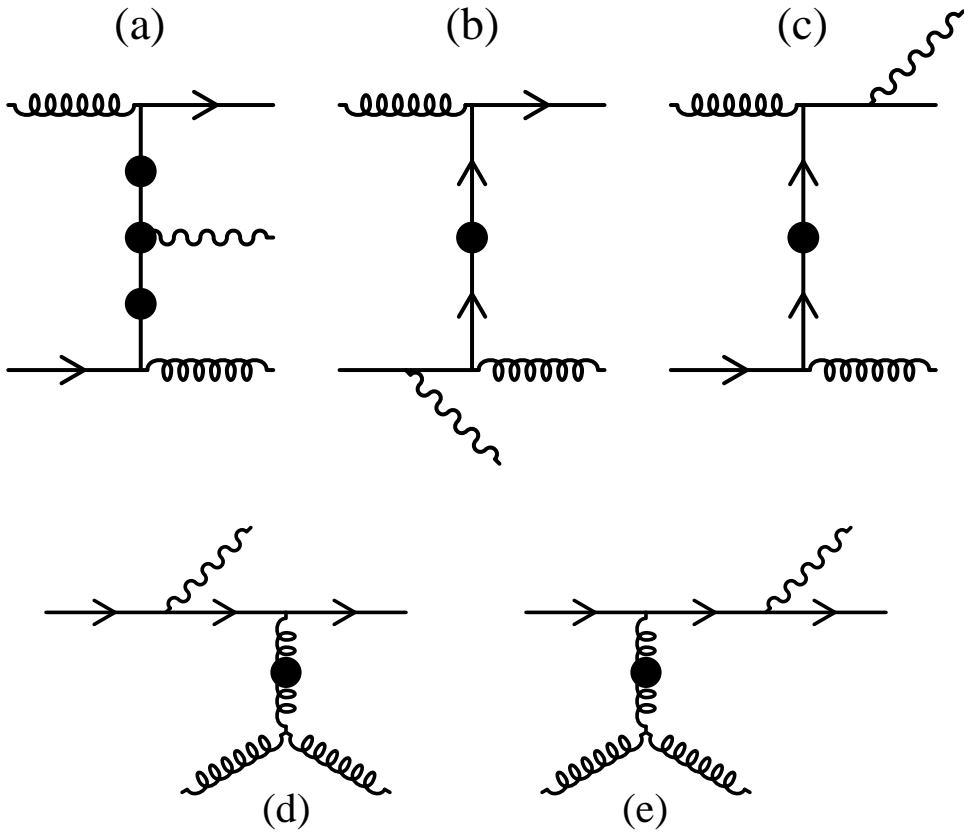


Figure 2: (a),(b),(c): matrix elements contributing to the imaginary part of diagrams (a) and (c) in Fig. 1; (d),(e): matrix elements contributing to the imaginary part of the gluon tadpole diagram in Fig. 1. The solid dots indicate effective propagators or vertices. The emitted photon has momentum much less than  $T$ . The other lines carry hard momentum.

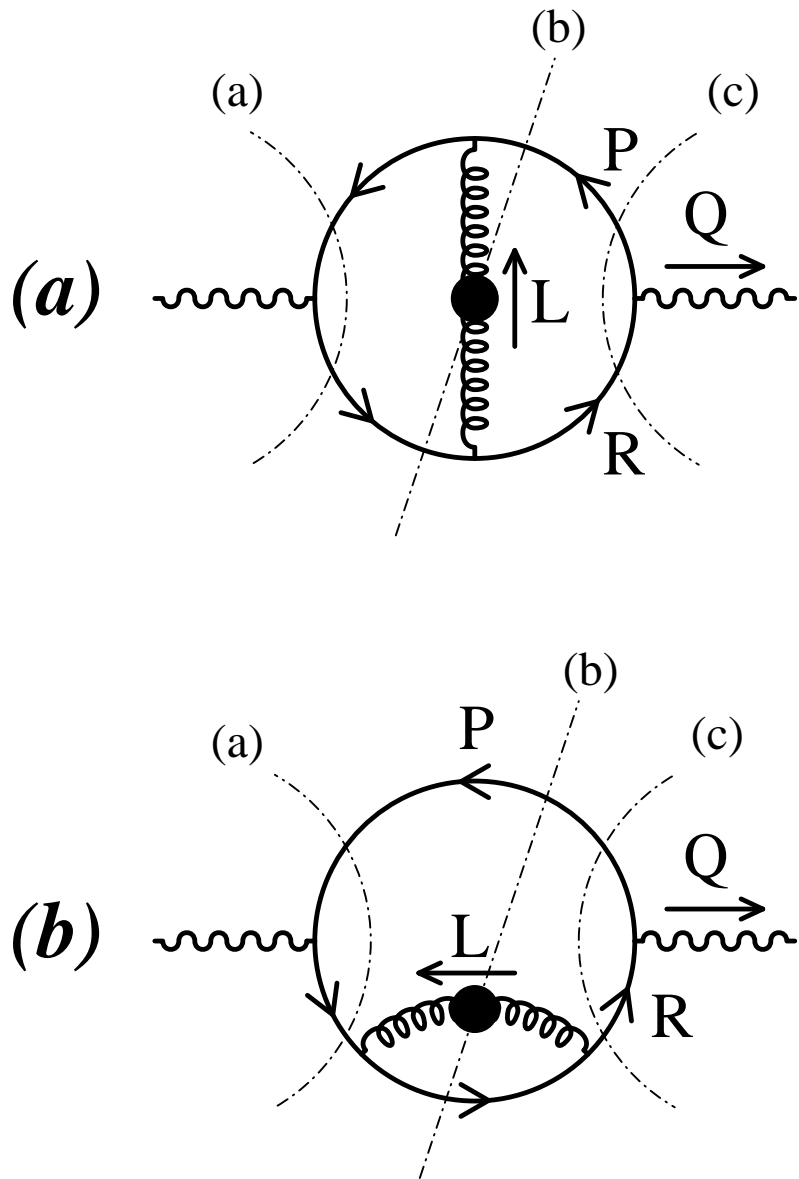


Figure 3: Contributions to the soft photon production rate with hard internal fermion lines – (a): vertex insertion; (b): self-energy insertion. The gluon propagator is an effective one. The fermion in the loop is hard.

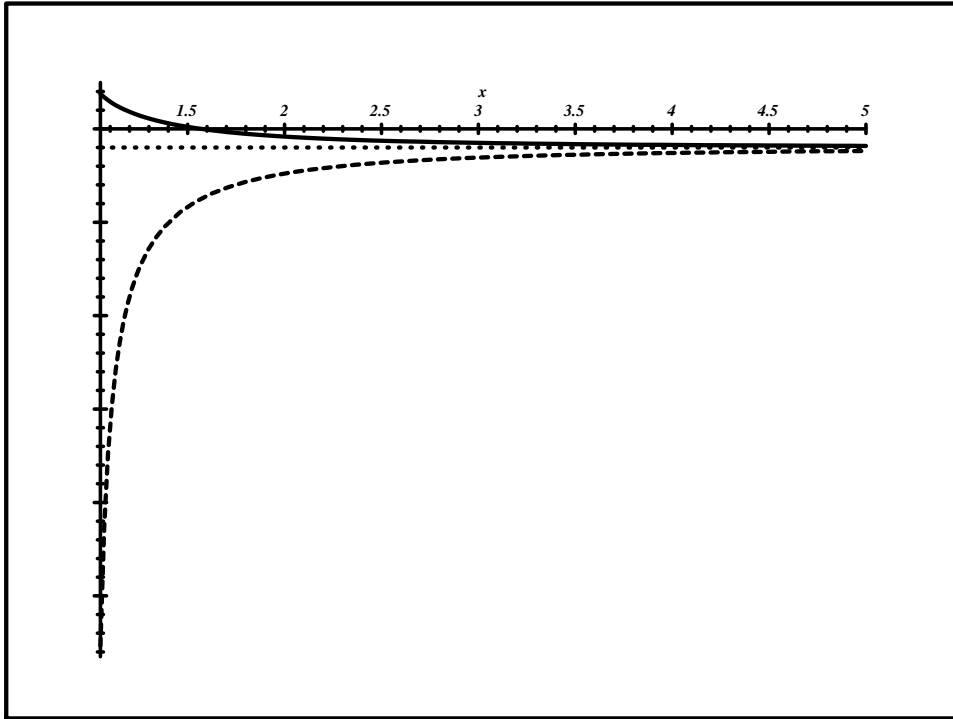


Figure 4: Solid line:  $1 - 4M_\infty^2 / \text{Re } \Pi_T(x)$ . Dashed line:  $1 - 4M_\infty^2 / \text{Re } \Pi_L(x)$ . Dotted line:  $1 - 4M_\infty^2 / m_g^2$ .

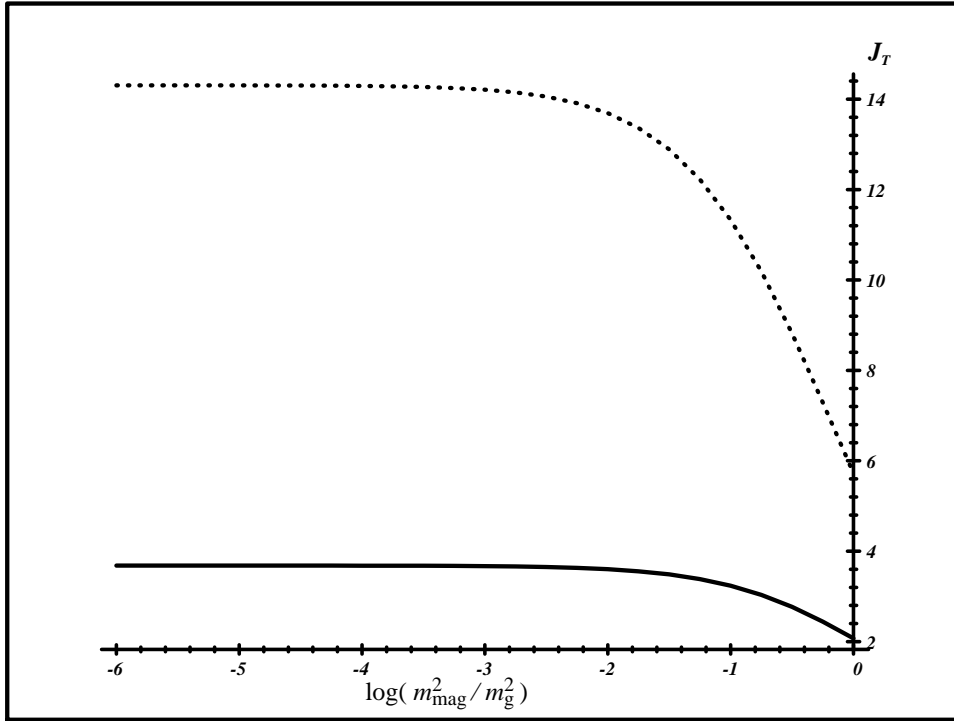


Figure 5: Effect of the magnetic mass on  $J_T$ . Solid line:  $(M_\infty/m_g)^2 = 1$ . Dotted line:  $(M_\infty/m_g)^2 = 0.1$ .

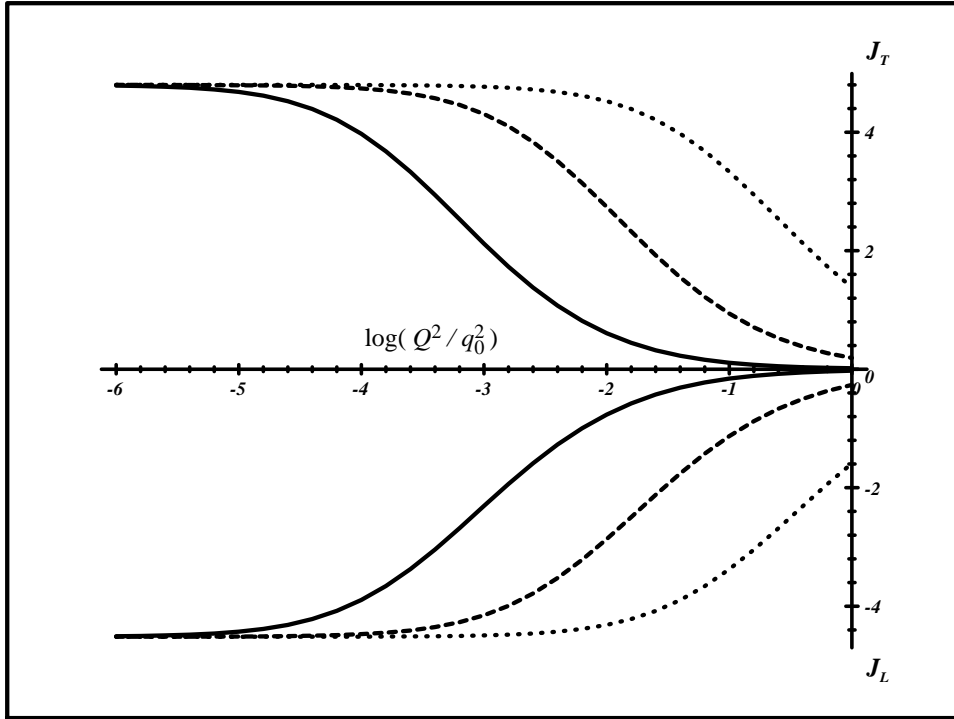


Figure 6:  $J_{T,L}$  as a function of  $\log(Q^2/q_0^2)$ , with  $(m_g/M_\infty)^2$  fixed to 1.5 (i.e.  $N = 3$  colors and  $N_f = 3$  light flavors). Solid curves:  $(m_g/T)^2 = 0.005$  or  $g = 0.1$ . Dashed curves:  $(m_g/T)^2 = 0.1$  or  $g = 0.44$ . Dotted curves:  $(m_g/T)^2 = 2$  or  $g = 2$ .